KAERI/RR-3749/2014

방사선 복합 생물반응 연구

Biological Responses to Combined Action of Radiation

2014. 12

한 국 원 자 력 연 구 원

제 출 문

미래창조과학부 장관 귀하

본 보고서를 “방사선 복합 생물반응 연구”의 보고서로 제출합니다.

2014. 12.

과제책임자 : 김 진 홍
참 여 자 : 김 진 규
참 여 자 : 김 동 호
참 여 자 : 노 창 현
참 여 자 : 정 동 민
참 여 자 : 강 미 영
참 여 자 : 류 태 호
참 여 자 : 장 은 영

요 약 문

I. 제 목

방사선 복합 생물반응 연구

Ⅱ. 연구개발의 목적 및 필요성

국가 방사선연구개발의 핵심기관인 한국원자력연구원 첨단방사선연구소는 인체 및 비인간 생물상에 대한 방사선방호 원천기술을 연구하고 관련 분야의 연구를 수행할 책무가 있다. 이를 위해서는 이온화 방사선에 대한 생물d,; 복합반응을 평가하고 검출하는 기술이 개발되어야 한다. 특히, 원자력 사고, 방사능 테러 및 방사선 이용의 증가 등에서 비롯되는 방사선 비상대응 기술로서의 방사선 생물방호 원천기술의 개발과 생물선량 평가기술 도약을 위한 노력이 필요하다. 방사선을 산업적, 과학적으로 이용함에 있어 생물학적 효용성을 증대시키기 위한 핵심기술로서 방사선과 물리·화학적 요인의 복합작용 심화연구를 수행하여 국제적 기술우위를 확보할 필요가 있다. 방사선과 다양한 물리·화학적 요인의 복합 생물반응을 검출하고 이를 응용할 수 있는 기술을 개발함으로써 국내 방사선 분야 기술우위를 확보하는 동시에 국가 경제발전에 기여할 임무를 맡고 있다. 또한 국제사회의 방사선 연구환경 변화와 생물방호 신개념에 부합하는 생물학적 선량평가 및 생물방호 원천기술을 확립하기 위한 연구가 요구되고 있다.

III. 연구개발의 내용 및 범위

본 연구개발에서는 다음과 같은 주요 내용과 범위가 연구개발에 포함되었다.

○ 방사선유발 염색체 이상 (dicentrics)을 이용한 생물선량 평가

○ 분자지표 (γ-H2AX)를 이용한 분자선량평가 기반연구
○ 방사선조사에 따른 세포신호전달 및 세포사멸 과정 분석연구
○ 방사선 노출에 따른 세포생존율 측정 검증
○ 퀘세틴 및 배당체의 방사선 방호 검증 및 연구
○ 세포에 대한 고 LET 및 저 LET 방사선의 복합작용

Ⅳ. 연구개발 결과

1. 방사선유발 염색체 이상 (dicentrics)을 이용한 생물선량 평가

이온화 방사선은 염색체의 이상과 DNA의 절단을 유발한다. 방사선 피폭 시 빠른 선량평가와 치료방향 결정을 위해 다양한 세포유전학적 검사들이 수행되고 있다. 그 중 말초혈액으로부터 분리된 림프구를 배양시켜 동원체의 개수를 확인하는 이동원체 분석법은 가장 널리 사용되고 있는 기법이다. 또한 이동원체 분석법은 미소핵 분석법이나 PCC 분석법에 비해 시간이 오래 걸리고 숙련된 기술을 요구한다는 단점이 있지만, 방사선 이외의 다른 인자들에 의해 영향을 덜 받고 노출 후 몇 년이 지나도 분석이 가능하다는 특이성 때문에 생물학적 선량평가에 여전히 중요하게 적용되고 있다. 방사선에 의해 발생하는 세포 핵 내 염색체 손상은 크게 안정형 염색체 이상과 불안정형 염색체 이상으로 나누어지는데, 본 연구에서는 불안정 염색체 이상을 관찰하는 이동원체 분석법을 통해 인간 말초혈액의 체외 감마선 조사 후 선량에 따른 변화를 확인하였다. 이동원성 염색체 이상을 분석하기 위해 건강한 성인 남녀 5 명의 말초혈액을 채취하고, 0 ~ 5 Gy의 감마선 (^{60}Co source, 42.6 TBq; AECL, Canada at Korea Atomic Energy Research Institute)에 세포를 노출시켰다. 총 21,688 개의 중기 세포를 관찰하여 10,969 개의 이동원성 염색체와 563개의 동원성 링, 그리고 11,364 개의 무동원체 절편을 발견했다. 방사선을 조사하지 않은 0 Gy를 포함한 모든 실험군에서 염색체 이상이 발견되었는데 세포 1,000 개당 1-2 개 정도의 이동원체는 백그라운드 빈도에 포함되므로 정상적이라고 볼 수 있으며, 이는 자연 방사선원으로부터의 노출에 의한 것으로 추정할 수 있다. 이동원체를 지닌 염색체의 발생 빈도수는 0에서 5 Gy까지 선량이 증가할수록 함께 증가하는 경향을 보여주었다. 이를 전통적인 선량-반응식으로 나타내면 $Y = 0.0123 + 0.2106D + 0.0249D^2$ (r^2=0.99)이라는 함수식으로 나타낼 수 있

다 (Y는 DC 염색체 수, D는 방사선량). 이 연구를 통해 방사선 선량에 따른 불안정 염색체 이상을 관찰하고 선량-반응 표준 곡선을 제작할 수 있었으며, 본 실험실에서의 이동원체 분석을 이용한 생물학적 선량평가 수립 가능성을 확인할 수 있었다.

2. 분자지표 (γH2AX)를 분자선량 평가 기반연구

생물체가 받은 방사선을 분자지표를 이용하여 평가하기 위하여 γH2AX를 분석을 수행하였다. 방사선에 의해 DNA 이중나선이 손상을 입게 되면 히스톤 단백질인 H2AX의 139번 위치의 serine이 급격히 인산화를 일으킨다. 이렇게 인산화된 형태인 γH2AX는 항체를 이용한 면역현광염색으로 검출할 수 있기 때문에 DNA 손상지표로 이용될 수 있다. 분자지표 γH2AX를 이용한 선량평가 기법을 확립하기 위하야 사람 유방암세포주인 MCF-7 세포를 이용한 실험을 수행하였다. 배양한 세포에 0 ~ 10 Gy의 감마선을 조사하였다. 조사된 세포를 면역형광염색법으로 염색하여 방사선 조사에 의하여 유발된 γH2AX foci를 방사선 조사 후 시간경과 별 (0, 0.25, 1, 2 및 24 시간)로 계수하였다. 방사선 조사 15분 경과 시 세포 당 foci 수는 대조군 (0 Gy) 12.4에서 10 Gy 조사군 56.0개로 선량증가에 따라 선형적으로 증가하는 양상을 나타내었다. 방사선 1 효 조사군을 기준으로 하였을 때 방사선 조사 후 2시간까지는 foci 수가 점진적으로 증가하였으나 24시간이 경과하고 나면 대조군의 기저값으로 감소하였다. 실험결과와 참고문헌을 통하여 볼 때 MCFG-7 세포에서의 γH2AX 유발양상은 발초혈액 림프구에서의 유발양상과 유사함이 확인되었다. 결론적으로, 방사선에 의해 유발되는 γH2AX foci 수는 선량에 비례적으로 증가하기 때문에 이를 측정하면 DNA 가닥 손상의 정도를 감시할 수 있을 뿐 아니라 암치료 환자에 있어서의 개인별 치료선량 결정을 위한 근거를 제공할 수 있다.

3. 방사선조사에 따른 세포신호전달 및 세포사멸 과정 분석연구

세포는 스트레스에 대하여 수복, 혹은 비가역적인 세포주기에서의 이탈과 세포예정사를 통한 제거 등 다양한 세포반응을 일으킨다. MCF-7 세포주와 HeLa 세포주를 이용하여 이온화 방사선에 의한 다양한 세포 반응에 대한 연구를 실시하였다. 방사선에 의한 세포반응

은 실험에 사용한 세포의 종류 (기원, 조직 및 발현되는 유전자 등) 와 가해진 세포 손상의 정도에 따라 다양하게 나타나며, 이러한 세포 반응의 이해는 세포의 운명, 즉 스트레스에 대한 세포 반응을 예상하고 결정하는데 중요하다. 세포는 DNA 손상에 따라 다양한, 일련의 세포 반응을 나타낸다. 그 중 p53/p21 경로의 활성화는 일시적으로 G1 혹은 G2 시기의 세포주기 억제를 야기하여 DNA 복제와 세포 분열을 종료시킨다. 활성화된 p53 은 p21 을 포함한 다양한 단백질의 발현을 유도하며 이는 세포주기 검문지점에서 세포주기 억제에 필요하다. 노화는 DNA 손상에 대한 세포 반응 중의 하나로, 이 반응 또한 p53/p21 경로의 활성화에 의해 촉진된다. 세포에서 DNA 손상에 의해 유도된 노화는 p53 의 활성이 특징적으로, 연이어 p21 이 축적되어 영구적인 세포주기 억제를 일으킨다. 세포예정사는 caspase라고 불리는 단백질 분해효소의 활성과 관련이 있으며, 정상 세포의 항상성과 조직의 발달에 필수적인 과정이다. 기존에 알려진 세포예정사인 아폽토시는 제 1 형 세포예정사로 명명되며 이와는 구분하여 제 2 형 세포예정사인 오토파지의 기전이 최근 활발하게 연구 중이다. 오토파지는 세포질 단백질과 세포 내 소기관들이 autophagosome 이라는 구조물에 싸여 라이소좀과 융합되는 과정이다. 많은 연구에서 방사선 조사에 의한 오토파지가 세포보호 기능을 한다고 보고되었다. 위에서 언급한 스트레스에 의한 세포 반응은 모두 방사선에 의해 유도된 p53 의 발현과 밀접한 관련이 있으며, 실험에 이용한 두 가지 세포에서 모두 이온화 방사선에 의해 증가된 수준의 p53 발현을 확인하였고, 그에 따른 세포 반응이 다르게 나타났다. 영구적인 세포주기 억제, 세포예정사 또는 오토파지가 p53/p21 경로의 활성화에 의해 일어난다. MCF-7 세포주는 p53 의존성 p21 의 활성화를 통해 G2/M 시기에서 세포가 arrest 되며 이로 인해 아폽토시스에 저항한다. 반면, MCF-7 세포는 SA-β-gal 활성을 나타내는 특징적인 노화의 양상을 보였다. 반면 HeLa 세포주는 G1 시기에서 세포가 arrest 되어 autophagic vacuoles (AVs) 의 염색 및 LC3-II 증가 등의 특성을 나타내는 오토파지의 양상을 나타냈다. 이와 같은 실험 결과에 따르면 이온화 방사선에 의한 세포 반응은 세포의 특성에 따라 다르게 나타나며, 그러한 다양한 반응의 이해는 세포 운명 결정 조절자로서 p53 의 기능 연구에 중요하다.

4. 방사선 노출에 따른 세포생존율 측정 검증

세포 생존율 측정은 방사선 치료에서 중요한 인자이다. 본 연구의 목적은 방사선 노출

후 MTT와 Trypan blue assay를 수행하기 위해 올바른 실험 조건을 제공하고자 한다. 방사선 노출에 대한 세포 생존율 측정을 위해 HepG2와 ^{60}Co 감마선을 이용하였다. 세포들은 96-well plates에 1 x 10^4 Cells/well 의 밀도로 깔고, 24시간 배양한 후, 1-100 Gy의 감마선에 노출하였다. 그 결과, Trypan blue assay의 경우, 방사선 선량의 크기가 증가함에 따라 세포의 생존율이 감소하였다. 하지만, MTT assay의 경우, 세포의 생존율에는 아무런 변화가 없었다. 이것은 96-well plates에서 1 x 10^4 cells/well 세포의 밀도는 MTT assay에 의한 세포 생존율 측정을 할때는 효과적이지 않다는 것을 의미한다. 따라서, 세포 생존율과 더 낮은 세포의 밀도 사이의 관계를 조사하였다. 그 결과, 최적의 세포 밀도는 1 x 10^4 Cells/well 이었다. 즉, 방사선과 관련된 실험에서 MTT assay를 사용할 경우 세포의 밀도가 아주 중요하다는 의미이다. 더불어, 세포 밀도에 따른 방사선 노출에 의한 세포 생존율은 clonogenic assay을 이용하여 검증하였다. 우리의 결과들은 방사선 노출에 의한 세포 생존율 측정을 위한 MTT assay와 Trypan assay는 clonogenic assay의 14일의 assay 시간보다 적게 걸리는 빠르게 측정하는 방법이라는 것을 제시하고, 두 assay을 이용하여 세포 생존율을 측정하기 위해서는 방사선 노출 후 적어도 3일이라는 배양시간이 필수적이라는 것을 제공한다.

5. 커큐민의 방사선 방어효과

커큐민은 울금에 함유된 폴리페놀로 항산화효능이 있다고 알여져 왔다. 따라서 본 연구에서는 사람 간암 세포주인 HePG2 세포를 실험모델계로 이용하여 커큐민의 효과를 연구하였다. 특히, 방사선 조사된 세포에 대해 세포보호 및 유전독성방호 효과가 있는지를 확인하고자 하였다. 방사선 조사에 따른 세포사멸과 DNA 손상은 Clonogenic assay와 Comet assay를 통하여 각각 분석하였다. 커큐민 0 또는 5 μM을 포함한 배지에 HePG2 세포를 2 시간 동안 배양한 다음 감마선 0~10 Gy를 조사하였다. 방사선 만을 조사한 실험군의 경우, 세포사멸과 DNA 손상이 방사선량의 증가에 따라 선형적으로 증가하는 것을 확인할 수 있었다. 반면에, 커큐민을 전처리 한 다음 조사한 실험군에서는 세포생존율이 높게 나타났을 뿐 아니라 DNA 손상도 낮게 나타났다. 이러한 실험결과에 비추어 볼 때 커큐민은 방사선의 영향에 변화를 일으키는 radiomodifier로 작용하여 세포보호 및 방사선방호 효과를 나타낸다는 결론을 얻었다.

6. 세포에 대한 고 LET 및 저 LET 방사선의 복합작용

방사선에 노출된 세포의 회복능력 자체가 변하지 않는 반면 재생이 불가능한 비가역적 손상이 증가한다는 새로운 해석은 방사선생물학계에 새로운 패러다임을 제공했다. 뿐만 아니라 방사선과 그 외 요인이 생물체에 복합 작용했을 때 유발하는 치사 손상과 준치사 손상에 대해 상승작용(시너지효과)은 두 부류의 준치사 손상끼리 상호작용을 통해 부가적 치사손상을 만들어내기 때문이라는 것을 이론으로 정립하였다. 생장 정체기에 달한 배수성 효모에 감마선과 알파선을 조사한 다음 생존율과 liquid-holding recovery (LHR)을 평가하였다. 조사된 세포가 잠재 치사손상으로부터 완전히 회복된 후 다시 방사선을 조사하고 피폭회복을 거치도록 하는 과정을 3반복하였다. 기존에 개발된 정량적 접근법을 이용하여 단위시간 당 회복확률과 세포의 비가역손상 분율을 산출하였다. 감마선 조사실험 결과, 세포손상의 비가역 분율은 초기 조사 때에 0.4였으나 3회 조사 후에는 0.7로 증가하였다. 고 LET 방사선인 알파선 조사 실험의 경우, 초기 조사 때 비가역손상 분율이 0.5에서 3차 조사 후 1.0으로 극명하게 증가하는 것으로 나타났다. 두 실험 모두의 경우 회복상수는 방사선 조사 횟수에 무관하였으나 방사선질의 영향을 약간 받는 것으로 밝혀졌다. 결론적으로, 저 LET나 고 LET 방사선 어느 경우나 세포가 반복조사 후 잠재 치사손상으로부터 회복되는 과정 자체는 변화됨이 없다. 따라서 방사선에 노출된 세포의 회복능력이 감소하는 것은 세포의 비가역손상 분율이 증가되기 때문인 것으로 해석될 수 있다.

Ⅴ. 연구결과의 활용계획 및 건의사항

이온화 방사선에 대한 생물반응 평가기술은 인간 및 생물상 보호를 위한 생물방호 원천기술로 자리 잡게 될 것이다. 중장기적으로는 방사선 작업종사자 및 사고 피폭자에 대한 생물반응의 회고적 선량평가에 필요한 생물반응 검출 기술의 수립에 활용될 것이다. 한편, 이온화 방사선과 또 다른 물리·화학적 요인의 복합 생물영향을 평가하기 위해 수립된 이론모델과 해석기법은 다요인 복합처리 시 나타나는 생물영향의 최대작용 조건 등을 사전 예측하고 최적화하는 기술로 발전될 수 있기 때문에 방사선의 긍정적 이용효

율을 증가시키는데 기여할 것으로 판단된다. 본 연구를 통하여 방사선 복합 생물영향 해석 신기술 자립 및 방사선민감도 해석 자료 구축을 통한 과학기술 발전기여와 함께 국제 기술우위를 확보할 수 있을 것이며 향후 새로운 연구과제 도출 및 수행을 위한 동기부여 및 기술기반으로 활용될 수 있다. 또한 개발된 방사선 복합작용 해석 연구의 결과를 집대성한 전문서적의 발간을 통하여 방사선 이용기술의 효과를 최적화 할 수 있는 기틀을 마련하였다.

SUMMARY

Ⅰ. Title of Project

Biological Responses to Combined Action of Radiation

Ⅱ. Objectives and Necessity of Research

Korea Atomic Energy Research Institute, Advanced Radiation Technology Institute has a national mission of Research and Development of Nuclear Technology. Especially Advanced Radiation Technology Institute plays a pivotal role for research and development in radiation technology. This study focused on development of fundamentals for radiation applications based on the existing radiation technology, development of fundamental technology for protection of human beings and non-human biota, as well. For that purpose, analyses of radiomodification and establishment of biodosimetry techniques have been carried our in this study. Furthermore, studying the combined action of ionizing radiation with another physical and chemical factor on the biological systems could provide a clue for enhancing efficacy of radiation utilization in various fields of research and industries.

III. Work Scopes of Research

The research consisted of the following work scopes.

○ Dose estimation with chromosomal aberration (dicentrics) analysis
○ Study on the molecular dosimetry with radiation induced γ-H2AX foci
○ Cell signals and cell death after exposure to ionizing radiation
○ Evaluation of cell viability after irradiation with different assays

○ Radiomodification of curcumin - radioprotective effects

○ Cell responses to combined action of low and high LET radiations

IV. Results of Research

1. Dose estimation with chromosomal aberration (dicentrics) analysis

The dicentric chromosome assay is very sensitive and a reliable bio-indicator in cases of accidental overexposure. The purpose of the present experiment was to provide data on the dose-dependent production of chromosome aberrations such as dicentrics, centric rings, and excess acentrics. To establish the control dose response curve that is appropriate for our laboratory, external gamma radiation was provided by a ^{60}Co source (42.6TBq of capacity; AECL, Canada at Korea Atomic Energy Research Institute). The healthy five donors were recruited to establish the dose-response calibration curve for unstable chromosomal aberrations by ionizing radiation exposure. The metaphases of human peripheral blood lymphocytes were analysed, after *in vitro* irradiated with gamma rays. In a total of 21,688 analyzed metaphase spreads, 10,969 dicentric chromosomes, 563 centric rings and 11,364 acentric chromosomes were found. The number of metaphase cells decreased with increasing radiation dose. The centric rings were not found at a 0 Gy dose, futhermore, there was not related with dose variation. The dose response curves were fitted to a linear quadratic model: $y = c + \alpha D + \beta D^2$, where y is the frequency of dicenrics, c is the background frequency, α is the linear component of the curve, β is the quadratic portion of the curve and D is the dose. The resulting dose-response calibration curve pooled from the five donors showed a classical linear-quadratic shape. The curve was fitted to the observed frequencies of dicentrics, in the doses range from 0 to 5 Gy. The fitted coefficients were $Y = (0.0123\pm0.0578) + (0.2106\pm0.0544)D + (0.0249\pm0.0104)D^2$ (r^2=0.99). The chromosomal aberrations such as dicentric, centric ring and acentric fragment were not founded in non-irradiated lymphocyte. The dose-related increase of the number of chromosomal

aberrations was observed. In particular, 5 dicentrics and the tricentric chromosomes were found in cells irradiated with 5 Gy. This study demonstrated that the production of dicentrics in human lymphocytes was intimately related with the irradiation dose. Therefore, these cytogenetic analyses will be helpful to a dose estimation after radiation exposure.

2. Study on the molecular dosimetry with radiation induced γ-H2AX foci

Upon DNA double-strand breaks (DSBs) induction, H2AX becomes rapidly phosphorylated at serine 139. This modified form, termed γ-H2AX, is easily identified with antibodies and serves as a sensitive indicator of DNA DSBs formation. The purpose of this study was to investigate the responses of human breast cancer cells to ionizing radiation by detecting γ-H2AX foci. Human MCF-7 breast carcinoma cells were irradiated with 0, 1, 5 and 10 Gy of γ-rays. Immunofluorescence staining was performed to score the number of radiation-induced γ-H2AX foci in the cells after irradiation. The foci were analyzed 0, 0.25, 1, 2 and 24 h after irradiation. The number of foci per cell 15 min after irradiation increased linearly with radiation dose; 12.4, 24.0, 41.2 and 56.0 for 0, 1, 5 and 10 Gy, respectively. The linear dose-response relationship was established from the result. In case of 1 Gy exposure, the number of foci gradually increased with time until 2 hours after irradiation. However, the number decreased down to the control background value 24 hour after irradiation. The result indicated that the response of MCF7 to ionizing radiation as measured by γ-H2AX formation were similar to human peripheral blood mononuclear cells. *Conclusions*: The number of γ-H2AX foci increases with exposure dose. Measurement of the foci is a possible approach to monitor DSBs or DSB repair in cancer patients during treatment with radiotherapy as a way to personalize the dosing.

3. Cell signals and cell death after exposure to ionizing radiation

Cells respond to stress with repair, or are diverted into irreversible cell cycle exit (senescence) or are eliminated through programmed cell death (apoptosis). Here those cellular responses induced by Ionizing Radiation were analyzed. MCF-7 and HeLa cells were used to evaluate cellular responses after γ-irradiation. p53 expression level was increased in a dose-dependent manner in both cells. IR induced a drastic increase in expression of p21 in MCF-7 compared to HeLa cells. Cell cycle analysis using flow cytometry showed a significant accumulation in G2/M phase after treatment of MCF-7 with IR. Induction of p21 and G2 arrest by IR impeded apoptosis in MCF-7. Instead, irradiated MCF-7 cells displayed cellular senescence as measured by staining of senescence-associated β-galactosidase (SA-β-gal) activity. These data suggest that senescence-associated increase in p21 function in regulating cell fate decision of MCF-7 cells. However, the role of p21 in G2/M arrest induced by either DNA damage or p53 alone remains to be elucidated. In addition to apoptosis, there exists a type II programmed cell death (PCD), autophagy. Detecting LC3 is a reliable method for monitoring autophagy. Western blots for the conversion of LC3-I to LC3-II and monodansylcadaverine (MDC) staining were conducted in HeLa cells since apoptotic features as well as SA-β-gal activity were not detected under our irradiation condition. Autophagy in HeLa cells may play an important role in cell protection and can result in cell survival. Immunofluorescence of γ-H2AX, a marker for double strand breaks (DSBs), was evaluated to check whether the initiation of DNA damage response after γ-irradiation was intact in MCF-7 cells. Cellular responses following IR were different depending on cell type and extent of genomic injury. The understanding of an appropriate cellular stress response is of crucial importance in foreseeing the cell fate.

4. Evaluation of cell viability after irradiation with different assays

Cell viability is an important factor in radiation therapy and thus is a method to quantify the effect of the therapy. Materials and Methods: The viability of human hepatoma (HepG2) cells exposed to radiation was evaluated by both the MTT and

Trypan blue assays. The cells were seeded on 96 well-plates at a density of 1 x 104 cells/well, incubated overnight, and irradiated with 1-100 Gy. Results: The cell viability was decreased in a dose-and time- dependent manner when using the Trypan blue assay, but no significant changes in the response to dose could be detected using the MTT assay. It indicated that the MTT assay was not efficient at a cell density of 1 x 104 cells/well on 96 well-plates to determine cell viability. Subsequently, the relationship between cell viability and lower cell density (1 x 103, 3 x 103, and 5 x 103 cells/well) was investigated. A cell density of 1 x 103 was found to be the most effective when using the MTT assay. Results show that the cell density is most important when using the MTT assay in 96 well-plates to follow in radiation effects. Furthermore, the radiation-induced cell viability dependent on cell density was confirmed by using the traditional Clonogenic assay. Conclusion: Our results suggest that the MTT and Trypan blue assays are rapid methods to detect radiation-induced cell viability of HepG2 cells in about 3 days as compared with 14 days of assay time in the Clonogenic assay. To obtain accurate cell viability measures using both rapid assays, an incubation time of at least 3 days is needed after irradiation.

5. Radiomodification of curcumin - radioprotective effects

Curcumin, a major polyphenol in turmeric, has been reported as a potential antioxidant to protect against unexpectable radiation risk. The objective of this study is to investigate the radioprotective effect of curcumin using human hepatoma (HepG2) cells, an excellent cell model for studying cytoprotective and antigenotoxic effect of compounds. Cell survival and DNA damage were measured by the Clonogenic survival assay and the Comet assay, respectively. HepG2 cells were pretreated with and without 5 μM curcumin in the culture medium for 2 h before irradiation (0-10 Gy). Ionization radiation (IR)-induced cell damage (cytotoxicity and genotoxicity) of HepG2 cells was evidenced by the decrease of cell survival and the

increase of DNA damage in a dose-dependent manner in the IR alone group. In contrast, curcumin pretreatment enhanced the cell survival (%) and suppressed the level of comet parameters in the curcumin plus IR group. These results suggest that curcumin can protect HepG2 cells against IR-induced cell damage.

6. Cell responses to combined action of low and high LET radiations

It was also shown that the recovery process itself was not damaged after exposure to high-LET radiation, as well as the enhanced relative biological effectiveness (RBE) values due to the increased yield of irreversible radiation damage from which cells were incapable of recovering. Diploid yeast cells were irradiated with gamma-rays from ^{60}Co and alpha particles from ^{239}Pu in the stationary phase of cell growth. Survival curves and the kinetics of the liquid-holding recovery were measured. When the irradiated cells had completely recovered from potentially lethal damage, they were again exposed to radiation and allowed post-irradiation recovery. The procedure was repeated three times. By use of a quantitative approach, describing the process of recovery as a decrease in the effective radiation dose, the probability of recovery per unit time and the proportion of irreversibly damaged cells were quantitatively estimated. It was shown that the irreversible fraction of cell injury was increased after repeated exposures to gamma rays, from 0.4 after the first irradiation to 0.7 after the third exposure. The effect was more clearly expressed after exposure to densely ionizing radiation, the corresponding values being 0.5 and 1.0. In contrast, the recovery constant did not depend on the number of repeated irradiations and only slightly depended on radiation quality. It is suggested that the process of recovery from potentially lethal radiation damage itself is not impaired after repeated exposures to both low- and high-LET radiations, and the decrease in the ability of the cell to recover from radiation damage is mainly explained by the increase in the proportion of irreversibly damaged cells.

V. Plan for Use of the R&D Results

Strong motivation and RT-based biotechnologies necessary for the future R&D plans can be provided from the results of this research. An advanced analytical method was suggested for the combined action of ionizing radiation with another factor. Using the method, it is possible to predict in advance the maximum value of synergistic interaction and the conditions to achieve the maximum. The results of this study give a clues for establishment of important technology associated with enhancing positive efficacy of radiation applications. By elaborating the present research results, new technologies will be established for analysing the combined effects of radiation with another factor and radiosensitivity of organisms. In the long run, *de novo* biodosimetry techniques will be developed and it can play an important role for ARTI to be an internationally recognized radiation biology and biodosimetry laboratory.

CONTENTS

목 차

List of Tables

List of Figures

제 1 장 서 론

KAERI

제 1 장 서 론

방사선 이용기술을 효과적으로 발전시키고 학계, 산업계 등 관련 분야에서 필요로 하는 핵심 기반기술의 개발·보급은 물론 산업화에 필요한 응용기술을 개발하는 것이 방사선 연구개발 국가 주체인 한국원자력연구원 첨단방사선연구소의 임무이다.

생명과학 산업이 인간생활 본위의 주력 산업으로 떠오르면서 지금까지 확립된 방사선기술을 바탕으로 생명과학기술, 환경기술, 우주기술, 나노기술 등을 융·복합시킨 새로운 개념의 과학 기술과 신제품을 개발하고자 하는 노력에 가속도가 붙기 시작하였다.

모든 생명체는 인공 및 자연 방사선과 여러 가지 물리·화학적 요인의 영향을 동시에 받으면서 살고 있다. 다양한 산업 분야에서 이온화 방사선이 가지고 있는 특성을 긍정적 이용하기 위한 노력이 증대되고 있으며 방사선과 기타 물리·화학적 요인이 복합적으로 생물체에 미치는 영향을 연구하고 해석하는 기술을 수립하고 응용하기 위한 기술개발이 시도되고 있다. 지금까지 방사선의 단순 조사 위주로 이용해 오던 평면적 기술에서 탈피하여 방사선 기술을 기반으로 하여 생명과학기술, 환경기술, 정보기술, 문화기술 등을 복합적으로 활용하여 한 차원 높은 방사선 융·복합 기술을 개발할 필요가 있다.

국제원자력기구, 국제방사선방호위원회 등은 새로운 방사선 생물방호를 위한 새로운 개념과 변화된 가이드라인을 제시하고 있기 때문에 이에 부합하는 연구 파라다임의 변화가 요구되고 있다. 또한 원자력 시설의 비상 사고나 테러 발생 시의 대규모 피폭자 및 희생자에 대한 생물선량평가 및 생물반응 검출기술 개발과 방사선 복합작용 해석 기술을 개발하기 위한 노력이 선진국 및 국제기구 (IAEA, EU, WHO, NATO 등)를 중심으로 다자간 협력연구가 활발히 진행되고 있는 상황임을 감안할 때 본 연구의 중요성이 인정된다.

지금까지의 방사선 연구는 대부분 실용기술 개발 또는 사안 대응을 염두에 둔 연구개발이 주류를 이루고 있었으나 장기적 산업경쟁력과 직결되는 기초원천 기술개발이 매우 취약한 상태이다. 국내에서는 여러 대학교가 방사선 연구를 수행하고 있으나 대부분 방사선치료와 관련된 연구 또는 단순 방사선 조사이용 연구에 국한되어 있는 것이 사실이다. 이에 한국원자력연구원 첨단방사선연구소를 중심으로 방사선 생물반응 평가 및 biophysics 원천기초 연구에 박차를 가하고 있다. 세계 선도그룹과 기술격차가 없거나 한국이 기술우위에 있는 “방사선 복합작용 연구” 부문을 창의적이고 도전적인 내용을 강화하여 세계적 기술우위를 유지하기 위한 노력을 기울이고 있다.

방사선 융합기술을 이용하여 생물선량 평가에 활용 가능한 기반기술을 수립하는 한편 방사선의 biophysics 연구를 수행하여 방사선의 긍정적 이용효율을 극대화하기 위한 체계 정립을 이뤄 국제적인 기술우위를 확보할 필요가 있다. 방사선 융합기술을 확립하여 방사선 이용의 새로운 장을 마련함으로써 국민의 삶의 질 향상에 기여하는 한편 국가 경쟁력을 높이는 계기를 마련하고자 한다.

연구 추진 전략으로는 방사선 연구의 국가 주체로서 방사선생물방호의 근간이 되는 방사선 복합생물반응 해석 기술을 개발하고 국제적 기술 주도권을 확보하기 위해 창의적 과제 추진과 국가적 임무를 성실히 이행할 것이며, 방사선 연구의 국제적 환경 변화와 연구 파라다임의 변화에 대응하고 원자력비상사고 및 테러 등에 대비한 방사선 생물방호 원천기술의 개발 필요성에 부응하기 위하여 장기적으로는 국제원자력기구의 지원과 공조로 방사선 복합생물반응 해석기술 및 생물방호 원천기술 수립을 통해 생물선량 평가 분야의 국제공조를 맞출 것이다. 방사선 생물반응 검출 기술은 방사선 뿐 아니라 식품, 환경 등에서 유래되는 유해인자에 대한 생물반응 검출에 직접적인 응용이 가능하므로 향후 환경부, 보건복지부, 농림축산식품부 등 타 부처와 기업체 과제의 수주에도 활용할 수 있을 것으로 전망된다.

제 2 장 본 론

KAERI

제1절 방사선유발 염색체 이상 (dicentrics)을 이용한 생물선량 평가

Dose estimation with chromosomal aberration (dicentrics) analysis

1. Introduction

Ionizing radiation causes chromosome breakages and produces cytogenetic aberrations in exposed cells [1-1]. In an investigation into radiation emergencies, it is important to estimate the dose to exposed persons for several reasons. Physical dosimeters (e.g., film badges) may misrepresent the actual radiation dose and may not be available in a radiological accident or terrorism incident. Biological dosimetry using chromosome aberration analysis in human peripheral blood lymphocytes (HPBL) is suitable and useful tool for estimating the dose when a nuclear or radiological emergency is investigated [1-2 ~ 1-4]. The unstable chromosome aberrations, such as dicentric and polycentric chromosomes, centric rings and acentric fragments are specific products of genome rearrangement after exposed to ionizing radiation [1-1, 1-5].

The conventional analysis of dicentric chromosomes in HPBL was suggested by Bender and Gooch in 1962 [1-6]. This assay has been for many years, the golden standard and the most specific method for ionizing radiation damage [1-4]. The dicentric assay technique in HPBL has been shown as the most sensitive biological method and reliable bio-indicator of quantifying the radiation dose [1-7].

The aim of our study was to establish the dose response curve of radiation-induced chromosome aberrations in HPBL by analyzing the frequency of dicentric chromosomes.

2. Materials and Methods

Chemicals

RPMI-1640 medium, fetal bovine serum, 100 UI/ml penicillin and 0.1 mg/ml streptomycin were purchased from Cellgro (USA). Giemsa solution was purchased from Merck (Germany). Rests of the chemicals were purchased from Sigma-Aldrich (USA).

Blood collections and irradiation

The blood donors were two healthy males (aged 27) and three females (aged 24, 25 and 26) without occupational exposure to harmful agents. The venipuncture heparinized whole blood sample from the five donor was divided into six containers (one group as a control and the others for exposure to 1, 2, 3, 4 and 5 Gy gamma rays). The samples were placed into a water bath and incubated at 37℃ for 1 hr immediately after irradiation in vitro at room temperature for 5 minutes by ^{60}Co source (42.6 TBq of capacity; AECL, Canada at Korea Atomic Energy Research Institute).

Dicentric analysis

Dicentric analysis was performed by the cytogenetic procedure [1-8]. The whole blood cultures were prepared by adding 0.3 ml blood to 4 ml RPMI-1640 medium to which antibiotic and bromodeoxyuridine have already been added. 10% fetal bovine serum and 100 μl phytohemagglutin (PHA-M) was added to mitosis and stimulate the lymphocyte proliferation. The blood samples were incubated in a cell culture flask (25 cm^2) at 37℃, 5% CO_2 in humidified atmosphere for 45 hours. Following incubation, a 50 μl colcemid solution was added to the culture and shaken gently. This culture was maintained for 3 more hours to provoke mitotic arrest.

After lymphocyte culturing, cells were harvested by centrifugation (200 g, for 10 min) and treated with 0.075 M potassium chloride solution to lyse the red blood cells. The lymphocytes were fixed with Carnoy's solution, a mix of methanol : glacial acetic acid (3 : 1). The cells were washed twice with a fixative solution, and the cell suspension from each sample was then dropped onto a wet clean glass slide. The slides were stained with a fresh Giemsa solution and allowed to dry. Finally, the slides were mounted in DPX.

Stained slides were scanned methodically at 200 fold magnification so that the entire area is covered. Once good quality metaphases were selected, dicentric analysis was conducted at high magnification (1,000 x). For a dicentric analysis, complete metaphases with 46 centromeres were recorded. If the cell contains unstable aberrations, it should

then balance. Tricentric aberrations are equivalent to two dicentrics and should have two accompanying fragments, while quadricentrics will have tree fragments, and so on.

Statistical Analysis

The difference between donors was tested using the Student *t*-test for comparing frequencies. Significant differences were defined at $p < 0.05$. For analysis of the dose-effect relationship, the calibration curve was fitted by least-square regression analysis to a linear-quadratic model using the Microsoft Office Excel 2010 and SigmaPlot 9.0. The 95% confidence intervals on the fitted curve were calculated assuming Poisson distribution. The standard *u*-test described by Papworth adopted by Savage [1-9] was used to test the goodness-of-fit for poisson probabilities. The variance (σ^2) by mean (y) ratio was used to test for Poisson distribution. Values of < 1 indicate underdispersion while values >1 indicate overdispersion. The *u*-values are included between ± 1.96, thus if the size of u value is out of that range, the dispersion of chromosome aberration yield is significant at 5%.

$$u = (\sigma^2/y - 1)\sqrt{\frac{N-1}{2(1-1/x)}}$$

where N is the number of cells analysed, and x is the number of chromosome aberrations detected.

3. Results and Discussions

The metaphases of HPBL were analysed, after *in vitro* irradiated with gamma rays. Table 1-1 shows the number of cells scored, the dicetrics, the centirc rings and the excess acentrics in each individual. The control (non-irradiated) samples in donor B, C and D include dicentric chromosomes, and it was regarded as the background frequencies. Several studies have been performed to evaluate the background frequencies of dicetric chromosomes [1-10]. Background dicentric frequencies from the healthy individuals are reported that between 0.09 [1-11] and 2.99 [1-12] per 1,000 cells.

The results indicate that the number of metaphases, dicentrics, centric rings, and acentrics in a dose-dependent manner at each individual.

Pooled data of dicentric, centric ring and acentric chromosomes of five donors are given in Table 1-2. In a total of 21,688 analyzed metaphase spreads, 10,969 dicentric chromosomes, 563 centric rings and 11,364 acentric chromosomes were found. The number of metaphase cells decreased with increasing radiation dose. The number of dicentric, centric ring and acentric chromosomes in the high-dose irradiation group were higher than in the low-dose irradiation group. The centric rings were not found at a 0 Gy dose, futhermore, there was not related with dose variation.

Table 1-3 shows the number of cells scored, the distribution of dicentric chromosomes among scored cells, the frequency of dicentrics (dicentrics per cell), the dispersion index (σ^2/y) and the u values. The distribution of dicentric chromosomes in the cells follows a Poisson distribution for most of the radiation dose points, although there was a trend toward underdispersion ($u < -1.96$).

Fig. 1-1 shows the results of chromosomal aberration frequencies among the five individuals and presents the appropriate dose-response curve of observed the dicentrics plus centric rings per cell. Although studying more individuals is necessary to ensure the data reliability and accuracy, these results are sufficient to generalized in most cases [1-13]. The dose response curves were fitted to a linear quadratic model: $y = c + \alpha D + \beta D^2$, where y is the frequency of dicenrics, c is the background frequency, α is the linear component of the curve, β is the quadratic portion of the curve and D is the dose. The fitted coefficients were $Y = (0.0290\pm0.0612) + (0.1870\pm0.0576)D + (0.0356\pm0.0111)D^2$ (r^2=0.99).

The resulting dose-response calibration curve pooled from the five donors showed a classical linear-quadratic shape (Fig. 1-2). The curve was fitted to the observed frequencies of dicentrics, in the doses range from 0 to 5 Gy. The fitted coefficients were $Y = (0.0299\pm0.0714) + (0.1738\pm0.0671)D + (0.0343\pm0.0129)D^2$ (r^2=0.99).

Fig. 1-3 shows an example of metaphases from human peripheral blood samples irradiated with from 0 to 5 Gy gamma rays. The chromosomal aberrations such as dicentric, centric ring and acentric fragment were not founded in non-irradiated

lymphocyte. The dose-related increase of the number of chromosomal aberrations was observed. In particular, 5 dicentrics and the tricentric chromosomes were found in cells irradiated with 5 Gy.

4. Conclusions

The healthy five donors were recruited to establish the dose-response calibration curve for unstable chromosomal aberrations by ionizing radiation exposure. Our cytogenetic results revealed that the mean frequency of chromosome aberration increased with increasing radiation dose. In this study, we suggested *in vitro* dose-response calibration curves for dicentric chromosomes in HPBL for ^{60}Co gamma rays. Additionally, our results support the previous study showing that the dose-response relationship for the production of micronucleus has established from a cytokinesis-block micronucleus assay [1-14].

Table 1-1. Results of chromosomal aberrations following *in vitro* irradiation of human peripheral blood from five donors

Experimental group	Age/Sex	Number of cells scored	Number of dicentrics	Number of centric rings	Number of excess acentrics
Donor A	26/F				
0 Gy		1156	0	0	0
1 Gy		1014	407	51	379
2 Gy		854	448	38	433
3 Gy		744	570	34	603
4 Gy		534	553	19	542
5 Gy		530	769	87	924
Donor B	25/F				
0 Gy		1187	2	0	2
1 Gy		716	120	7	126
2 Gy		506	198	14	208
3 Gy		299	215	13	227
4 Gy		288	294	16	302
5 Gy		194	350	22	358
Donor C	24/F				
0 Gy		1034	2	0	2
1 Gy		939	212	0	214
2 Gy		816	346	13	359
3 Gy		750	794	42	827
4 Gy		654	860	47	906
5 Gy		568	1068	29	1099
Donor D	27/M				
0 Gy		1014	2	0	2
1 Gy		930	245	15	245
2 Gy		645	360	15	375
3 Gy		579	591	15	606
4 Gy		309	354	27	381
5 Gy		219	402	9	411
Donor E	27/M				
0 Gy		1754	0	0	0
1 Gy		1595	390	0	386
2 Gy		1415	840	35	860
3 Gy		247	261	5	266
4 Gy		120	169	3	172
5 Gy		78	147	7	149

Table 1-2. Pooled data of chromosomal aberrations after *in vitro* irradiation of human peripheral blood from five donors

Dose (Gy)	Number of cells scored	Number of dicentrics	Number of centric rings	Number of excess acentrics
0	6145	6	0	6
1	5194	1374	73	1350
2	4236	2192	115	2235
3	2619	2431	109	2529
4	1905	2230	112	2303
5	1589	2736	154	2941

Table 1-3. Yield and intercellular distribution of dicentric chromosomes after in vitro irradiation of human peripheral blood from five donors

Dose (Gy)	Donor	Number of cells scored	Number of cells with dicentric chromosomes						Dicentrics per cell (y)	σ^2/y	u
			*d*0	*d*1	*d*2	*d*3	*d*4	*d*5			
0	A	1156	1156	0	0	0	0	0	0.000	0	0.00
	B	1187	1185	2	0	0	0	0	0.002	1.00	-0.03
	C	1034	1032	2	0	0	0	0	0.002	1.00	-0.03
	D	1014	1012	2	0	0	0	0	0.002	1.00	-0.03
	E	1754	1754	0	0	0	0	0	0.000	0	0.00
1	A	1014	726	179	99	10	0	0	0.401	1.23	5.23
	B	716	606	100	10	0	0	0	0.168	1.00	-0.02
	C	939	748	170	21	0	0	0	0.226	0.97	-0.60
	D	930	659	226	8	1	0	0	0.263	0.83	-3.73
	E	1595	1225	351	18	1	0	0	0.245	0.86	-3.86
2	A	854	501	271	73	6	2	1	0.525	0.98	-0.42
	B	506	320	175	10	1	0	0	0.391	0.74	-4.12
	C	816	490	306	20	0	0	0	0.424	0.69	-6.22
	D	645	300	330	15	0	0	0	0.558	0.53	-8.51
	E	1415	803	414	168	30	0	0	0.594	1.02	0.55
3	A	744	313	323	85	16	6	1	0.766	0.86	-2.66
	B	299	117	150	31	1	0	0	0.719	0.60	-4.91
	C	750	114	481	152	3	0	0	1.059	0.35	-12.63
	D	579	144	297	120	18	0	0	1.021	0.57	-7.34
	E	247	62	118	58	9	0	0	1.057	0.59	-4.49
4	A	534	106	327	80	19	1	1	1.036	0.52	-7.87
	B	288	71	154	49	14	0	0	1.021	0.60	-4.80
	C	654	40	382	218	14	0	0	1.315	0.29	-12.83
	D	309	75	138	78	12	6	0	1.146	0.70	-3.70
	E	120	8	61	45	6	0	0	1.408	0.34	-5.10
5	A	530	86	213	148	73	9	1	1.451	0.67	-5.36
	B	194	8	58	102	18	6	2	1.804	0.41	-5.81
	C	568	10	147	315	93	3	0	1.880	0.27	-12.36
	D	219	6	72	96	42	3	0	1.836	0.36	-6.69
	E	78	2	28	34	7	5	2	1.885	0.54	-2.82

d distributions of dicentrics in cells.

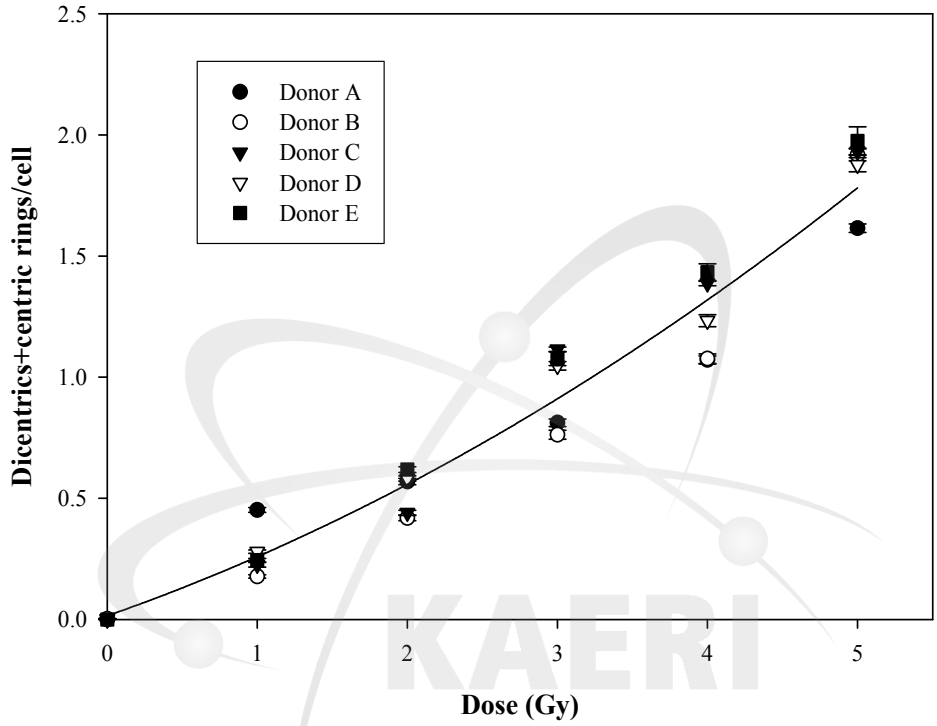

Fig. 1-1. Dose-response curve for chromosomal aberrations (dicentric chromosomes and centric ring chromosomes) induced by gamma rays in lymphocytes derived from five donors. The fitted values of the coefficients of the linear quadratic function $y = c + \alpha D + \beta D^2$: $c = 0.0149 \pm 0.0611$; $\alpha = 0.2165 \pm 0.0574$; $\beta = 0.0274 \pm 0.0110$. Error bars represent the standard error.

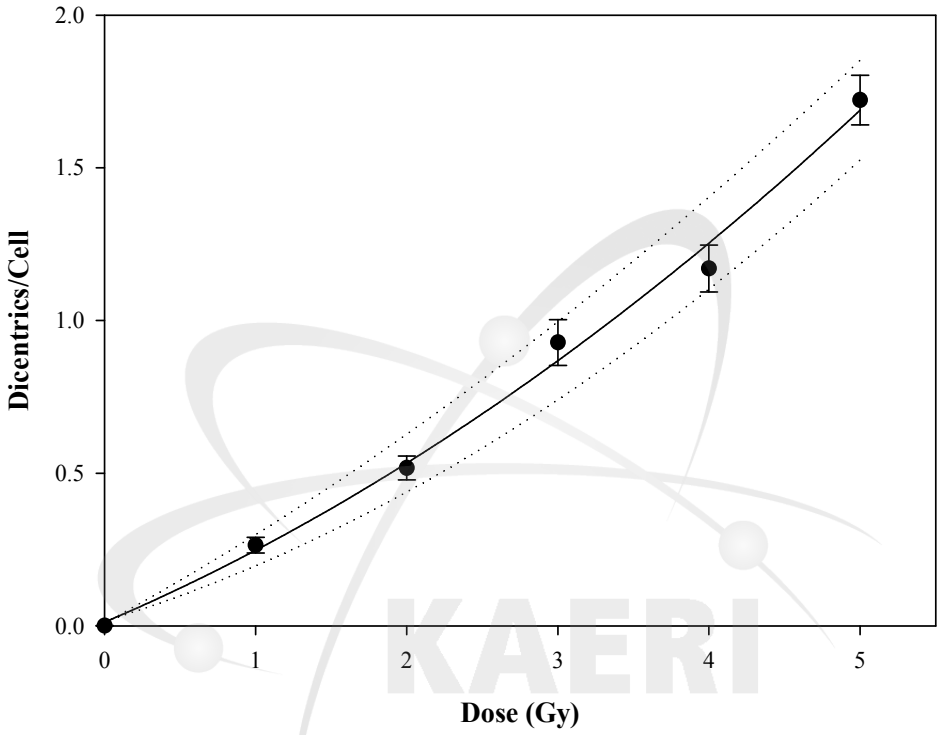

Fig. 1-2. Dose-response curve for dicentric chromosomal aberrations induced by gamma rays in lymphocytes derived from five donors. The fitted values of the coefficients of the linear quadratic function $y = c + \alpha D + \beta D^2$: c = 0.0123 ± 0.0578; α = 0.2106 ± 0.0544; β = 0.0249 ± 0.0104. Error bars represent the standard error. Dotted lines are the upper and lower 95% confidence intervals. Error bars represent the standard error.

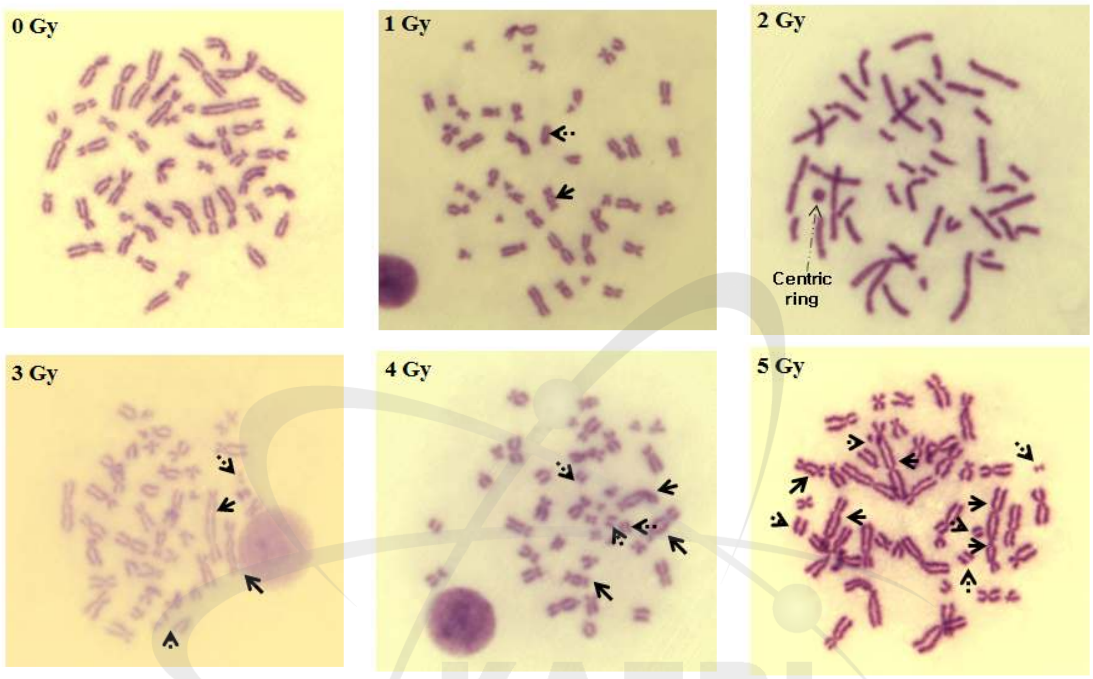

Fig. 1-3. The representative pictures of metaphase lymphocytes after irradiated with 0 - 5 Gy gamma rays at 1,000 magnification. Solid arrows are dicentric chromosomes and dotted arrows are acentric fragments.

제2절 분자지표 (γH2AX)를 분자선량 평가 기반연구

Study on the molecular dosimetry with radiation induced γ-H2AX foci

1. Introduction

H2AX is a histone H2A variant that constitutes 2-25% of mammalian histone H2A depending on the organism and cell type [2-1]. Upon DNA double-strand breaks (DSBs) induction, H2AX becomes rapidly phosphorylated at serine 139. This modified form, termed γ-H2AX, is easily identified with antibodies and serves as a sensitive indicator of DNA DSBs formation [2-2]. Physical techniques for monitoring DSBs require high, non-physiological doses and cannot reliably detect subtle defects. One outcome from extensive research into the DNA damage response is the observation of γ-H2AX foci that can be visualized by immunofluorescence. There is a close correlation between γ-H2AX foci and DSBs numbers and between the rate of foci loss and DSB repair, providing a sensitive assay to monitor DSB repair in individual cells using physiological doses [2-3, 2-4].

Dose assessments based on well established cytogenetic assays and especially those utilising emerging techniques in the field of biological dosimetry are time consuming, operator dependent and is not scalable for high throughput assay development. In contrast, many of the emerging biological dosimetry techniques, which focus on quick dose assessments [2-5]. γ-H2AX established immunocytochemical markers of ionizing radiation-induced DNA DSBs and are emerging biomarkers of radiation exposure. Their potential for accurately estimating radiation dose has already been reported [2-6, 2-7]. Those studies demonstrate excellent sensitivity down to a few milligray, the ability of the γ-H2AX assay to identify a recent partial body exposure, and persistence of foci for several days after high dose exposure [2-8]. The purpose of the present experiment was to investigate the responses of human breast cancer cell to gamma irradiation by detecting γ-H2AX foci and to make a standard dose response curve resulting in technical challenges in the development of specific analytical procedures.

2. Materials and Methods

Cell line and culture

Human MCF-7 breast carcinoma cell line aquired from American Type Culture Collection (Manassas, VA) was grown in RPMI 1640 supplemented with 10% Fetal Bovine Serum (FBS), antibiotic-antimycotic at appropriate concentration (all from GIBCO, USA) and 5 μg/ml plasmocin (InvivoGen, CA, USA) at 37 °C with 5% CO_2 in a fully humidified atmosphere.

DNA damage treatments

The samples were prepared for exposure to 1, 5 and 10 Gy gamma rays and immediately treated with increasing doses of ionizing radiations from ^{60}Co source (42.6 TBq, AECL, Canada at Korea Atomic Energy Research Institute) for 5 min at room temperature, respectively.

Immunofluorescence staining of γ-H2AX

To visualize nuclear foci, cells cultured on cover slips coated with poly-L-lysine (Sigma-Aldrich) had been maintained in culture medium in a 24 well culture dish for 24 h before treatment. Either untreated or irradiated coverslips were washed in PBS and then fixed in 100% cold methanol for 15 min at room temperature. Subsequently, cells were washed and permeabilized in PBS containing 0.01% (v/v) Triton X-100 (Sigma-Aldrich) for 15 min RT. Fixed and permeabilized cells were washed three times in PBS, and non-specific binding sites were blocked in PBS containing 0.1% BSA for 2 h RT, following which cells were incubated with anti-gamma H2A.X (phospho S139) antibody (Abcam; 1:500 dilution) in PBS containing 0.1% BSA at 4 ◦C overnight. Next, the cells were washed with PBS and then stained with donkey anti-rabbit IgG-FITC (Santa Cruz; 1:200 dilution) in PBS for 2 h RT, followed by washing in PBS. After washing, the cells were mounted using Vectashield mounting medium with 4, 6-diamidino-2-phenylindole (Vector Laboratories, Burlingame, CA, USA).

3. Results

The distribution of γ-H2AX in irradiated cells was examined. The human breast cancer cell line MCF7 responded to ionizing radiation with the formation of discrete foci containing γ-H2AX throughout the nuclei. Some cells contained foci in the absence of irradiation (Fig. 2-1).

Foci were apparent 15 min after irradiation with 1 Gy (Fig. 2-2B), persisted for 15-120 min (Fig. 2-2C. D), then decreased in number at 24 h (Fig. 2-2E). Mean number of γ-H2AX foci per cell following irradiation with 1 Gy gamma-rays according to incubation time was shown in Figure 2-3, in which individual nuclei in fields of cells were scored for the number of foci. Compared with the unirradiated control cells, which contained an average of 11.25 ± 1.79 foci per nucleus, MCF-7 cells 15 min after exposure to 1 Gy contained numerous small foci, with an average of 24.00 ± 2.69 foci per nucleus. The foci became more in number and better defined after 1 h, 29.80 ± 4.49 foci per nucleus; 2 h, 33.40 ± 3.32 foci per nucleus. The number of foci decreased to 18.00 ± 1.87 foci per nucleus at 24 h post-irradiation. Radiation-induced γ-H2AX foci represent DSBs. After 24 h recovery, the number of foci decreased, possibly suggesting that the introduced DNA DSBs had been rejoined.

γ-H2AX intensity, as measured by immunofluorescence, increased with dose in MCF7 cell exposed to 1, 5 and 10 Gy gamma rays. Larger amounts of radiation resulted in larger numbers of foci in MCF-7 (Fig. 2-4). In irradiated MCF-7 cell, mean number of γ-H2AX foci was linearly induced with doses of 1, 5 and 10 Gy at 15 min post exposure (Fig. 2-5). The values for 5 and 10 Gy are somewhat less than expected for linear proportionality with respect to the amount of radiation. This discrepancy may be partly explained if two foci at different levels in the nuclei overlap in the maximum projection and are scored as a single focus. This overlapping is more likely as the number of foci increases.

4. Discussion

Rogakou *et al.* (1998) have discovered that DSB produced by IR treatment triggered the phosphorylation of serine 139 in the carboxy-terminal domain of H2AX. Over the last several years, γ-H2AX expression has been established as a sensitive indicator of DSBs. Because the DSB is the critical lesion induced by ionizing radiation, their analysis provides essential insight into fundamental and translational radiobiology [2-10]. Assessment of the biologic response to radiation exposure is a straightforward application in the use of γ-H2AX as a biodosimeter [2-11].

The present study was aimed to set the standard procedure for detection of γ-H2AX foci. We show here, with MCF-7 cells, an average of 24.0 ± 2.69 foci per nucleus 15 min after exposure to 1 Gy. The γ-H2AX foci scoring obtained as shown in figure 3 and 5, was higher than that by Rogakou *et al.* (1999), in which the comparable numbers in MCF-7 cell were 12.2 ± 5.7 foci per nucleus 15 min after 0.6 Gy, and 27.1 ± 10.8 foci per nucleus 15 min after 2 Gy. γ-H2AX intensity evaluation, as measured by immunofluorescence under our laboratory exrerimental condition, was able to detect low levels of DSBs produced by ionizing radiation. Avondoglio *et al.* (2009) evaluated γ-H2AX using U251 cell (human glioblastoma cell line), and they showed the saturated foci count (~60) 1 h post-irradiation at dose from 4 Gy. As compared that results, the similar number of foci was obtained after 10 Gy exposure in the present experiment. In figure 5, the linear induction of γ-H2AX foci levels with dose observed shows that foci yields per gray were not constant; 5 and 10 Gy at 15 min post exposure foci counts for γ-H2AX didn't conform to linearity. This 'underscoring' of foci at high doses early after exposure was likely caused by the close proximity or even overlap of adjacent foci which makes it impossible to distinguish each individual focus using microscopy.

No mammalian cell line, normal or repair-defective, has been found that lacks the ability to form γ-H2AX when exposed to ionizing radiation [2-12]. Therefore, the standard method for foci scoring need to be set according to the characteristics (origin,

organism, genes expressed etc.) of cell line used. Detection of radiation-induced DSBs using γ-H2AX assay in MCF-7 cell, as shown in our data, could be utilized as a powerful tool for dose estimation.

γ-H2AX analysis has enhanced our ability to detect DNA damage in individual patients and opens for the first time the possibility to measure DNA-damage during cancer treatment and in bio-monitoring purposes in clinical laboratories. In addition, a wide range of genotoxic events can now be monitored in individuals with the γ-H2AX methods due to its unique sensitivity and tight correlation to the toxicity of the DNA-damage [2-13].

The obtained result that ~27 γ-H2AX foci were present in MCF-7 cell 1 h after exposure to 1 Gy gamma-rays (data was not shown) was similar to the yield of DSBs that is induced per Gy of gamma-rays in human cells. About 50 γ-H2AX foci 1 h after exposure to 2 Gy were observed in mononuclear cells by Johansson *et al.* (2011). This indicates that responses of MCF7 to ionizing radiation exposure, as measured by γ-H2AX formation, were similar to human peripheral blood mononuclear cells. One major consideration in γ-H2AX foci biodosimetry is the source of patient cells to be assayed after exposure to DNA-damaging agents. Thus, future experiments are planned to analyze different responses to irradiation from samples of various sources.

Measurements of γ-H2AX foci could therefore be a possible approach to monitor DSBs or DSB repair in cancer patients during treatment with radiotherapy or chemotherapy as a way to personalize the dosing. It is also possible that γ-H2AX measurements could be used for radiation biodosimetry for nuclear plant workers or in the general public after nuclear accidents as well as exposure to potentially DNA damaging environmental toxins.

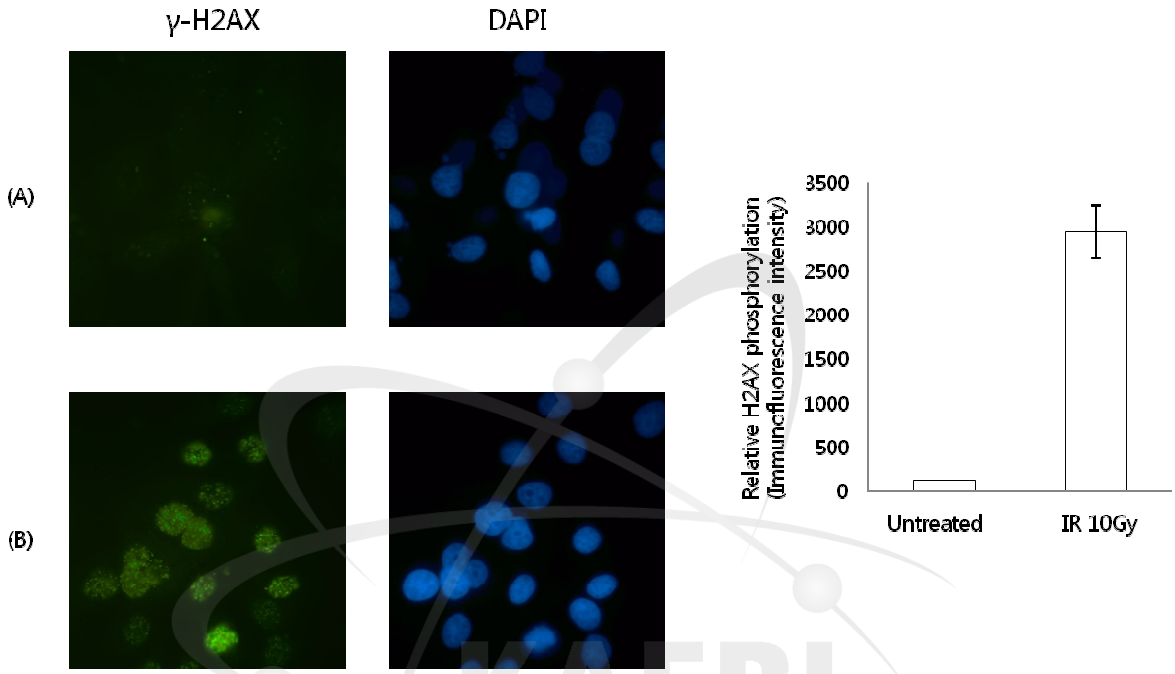

Fig. 2-1. Repregentative image of MCF-7 cells irradiated with 10 Gy gamma-rays at 1,000 fold magnification: (A) Untreated control, (B) γ-H2AX foci formation at 2 h post-irradiation. Relative H2AX phosphorylation intensity was calculated by ImagePartner 4.0 software.

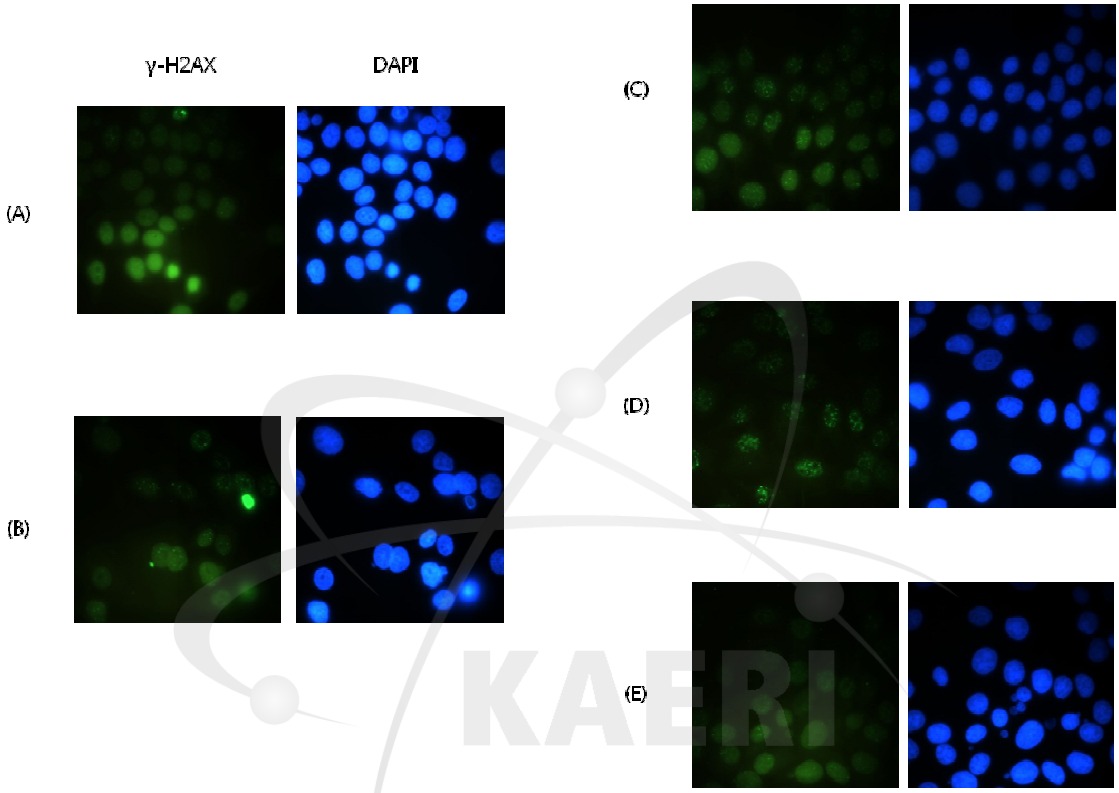

Fig. 2-2. γ-H2AX foci formation in MCF-7 cell after 1 Gy gamma-rays irradiation: (A) 0, (B) 15 min, (C) 1 h, (D) 2 h and (E) 24 h after irradiation.

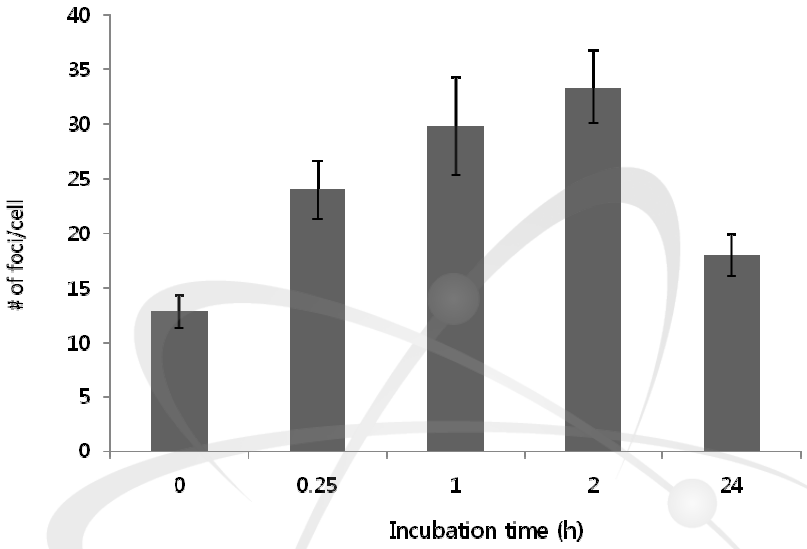

Fig. 2-3. The plot for the linear dynamic range of γ-H2AX foci per cell following irradiation with 1 Gy gamma rays.

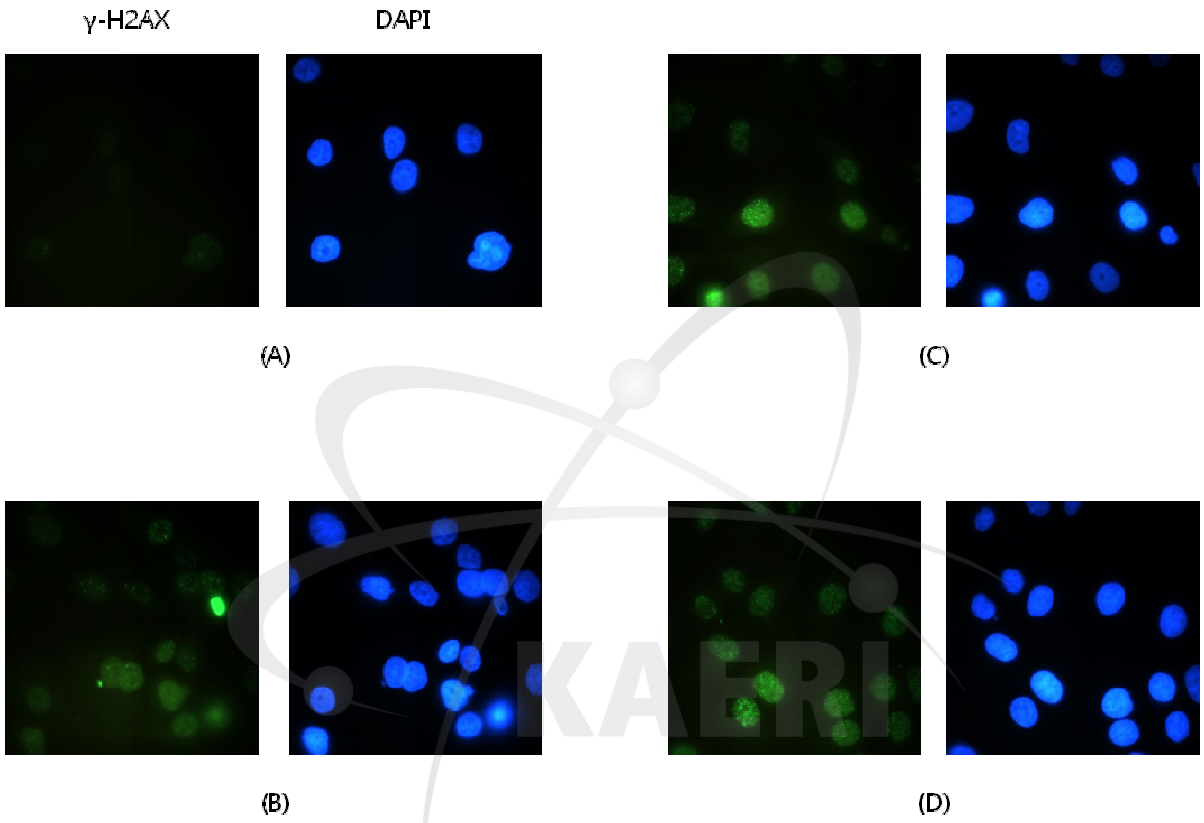

Fig. 2-4. γ-H2AX evaluation in MCF-7 cell at 15 min post-irradiation: (A) 0, (B) 1 Gy, (C) 5 Gy and (D) 10 Gy.

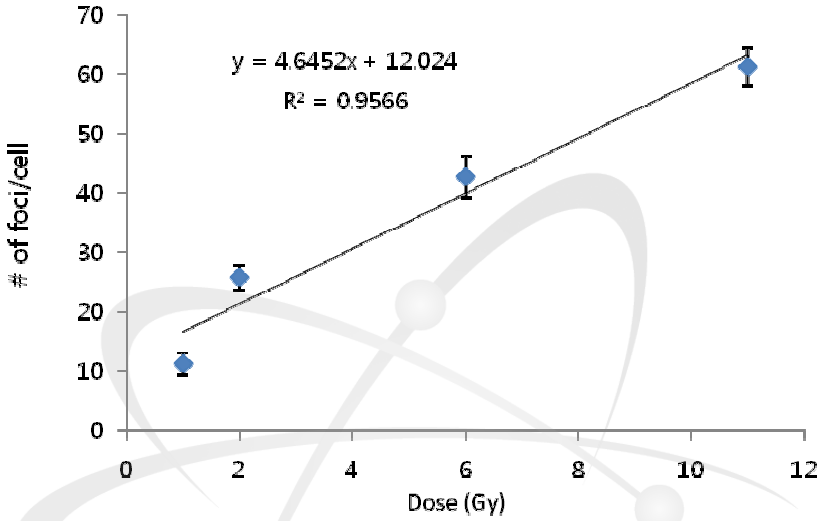

Fig. 2-5. Dose-dependence of γ-H2AX foci formation in MCF-7 cell at 15 min post-irradiation.

제3절 방사선조사에 따른 세포신호전달 및 세포사멸 과정 분석연구

Cell signals and cell death after exposure to ionizing radiation

1. Introduction

The wild-type p53 tumor suppressor regulates multiple signaling pathways triggered by diverse cellular stresses, including DNA damage [3-1]. In response to DNA damage, the p53 signaling network is activated to induce cell cycle arrest, apoptosis, or senescence depending on the type of genotoxic stimuli and the genetic background of the cells [3-2]. Activated p53 induces the expression of many proteins including p21, which is a universal inhibitor of the cyclin-dependent kinases (Cdks), and is required to arrest cells at the G1 and G2 checkpoints of the cell cycle after DNA damage [3-3].

The activation of p53 facilitates two major morphologically distinctive forms of programmed cell death. Apoptotic cell death is executed by a family of cysteine proteases, caspases, which lead to the demise of the cell [3-4]. Among them, caspase-3 activity has been detected in apoptosis induced by a variety of apoptotic signals, including ionizing radiation [3-5]. It is absolutely crucial for apoptosis induction, as this enzyme is not only activated downstreams of death path way, it is also responsible for the cleavage of the majority of substrates [3-6].

Autophagic cell death is another important physiological cell death process. Autophagy is an evolutionary conserved process whereby cytoplasmic proteins and cellular organelles are enveloped in autophagosomes and degraded by fusion with lysosomes [3-7]. Some autophagic cell death events might have been attributed to apoptosis. However, there is emerging evidence that autophagy plays a crucial role in the regulation of cell survival [3-8, 3-9]. Stress-induced premature senescence (SIPS), on the other hand, is a growth-arrested state in which the cells acquire flattened and enlarged morphology, express the marker senescence-associated β-galactosidase (SA-β-gal), and cease to synthesize DNA, but remain viable and secrete growth- and tumor-promoting factors [3-10].

The strategy to deal with damaged DNA in mammalian cells can be split into three

components: the recognition of injured DNA, a period of damage assessment, and the implementation of the appropriate response, DNA repair or cell death [3-11, 3-12]. Understanding how the decision between apoptosis and other fates can be made at checkpoints activated by DNA damage is of crucial importance.

It is known that p53 is involved in several biological functions [3-1]. Nevertheless, how p53 determines the fate of cells still remains as an important question. It has been shown in several cell types that p53 protein levels are correlated with cell fate decisions [3-13]. However, those cellular responses were induced by inhibition of p53 using p53 lentiviral-mediated expression of siRNA [3-14] or by overexpression of p53 with Ad-p53 infection [3-15] or TET-regulatable p53 expression system [3-16]. Cellular responses induced by artificial regulations of p53 protein levels showed critical features representing the function of p53, but it was far from the biological responses inside the cells.

This study was done to identify p53-mediated regulation, how the tumor suppressor p53 is involved in the complex responses to IR to enforce the cell's fate to live by inducing the growth arrest coupled to p53-induced autophagy or to die by inducing irreversible growth arrest, apoptosis at the physiological condition. In addition, to date, little is known about the role of autophagy in the molecular mechanisms that confer to cell protection and result in cell survival. Herein, the purpose of this study is to elucidate the influence of p53 status on cell fate, that is, a role of p53 in two fundamentally important cell biological pathways: autophagy and apoptosis.

2. Materials and Methods

Reagents

Reagents were obtained from the following sources: antibodies to p53, chk1, p21, PARP, cleaved PARP, β-actin and goat anti-mouse IgG-HRP and goat anti-rabbit IgG-HRP, from Santa Cruz (Santa Cruz, CA, USA); anti-cleaved caspase-3 and -7, from Cell Signaling (Beverly, MA, USA); LC3 antibody, from novus (Littleton, CO,

USA); poly-L-lysine, propidium iodide, acridine orange and 3-methyladenine, from Sigma-Aldrich (St. Louis, MO, USA); z-VAD-fmk from InvivoGen (San Diego, CA, USA); antibiotic-antimycotic and trypsin-EDTA, from Gibco-BRL (Gaithersburg, MD, USA); DMEM and fetal bovine serum (FBS), from Welgene (Daegu, Korea); senescence detection kit and caspase-3 colorimetric assay kit, from BioVision (Milpitas, CA, USA).

Cell culture and DNA damage treatments

Human HeLa cervical carcinoma cell line aquired from American Type Culture Collection (Manassas, VA) was grown in DMEM supplemented with 10% Fetal Bovine Serum (FBS), antibiotic-antimycotic at appropriate concentration (all from GIBCO, USA) and 5 μg ml^{-1} plasmocin (InvivoGen,CA,USA) at 37°C with 5% CO_2 in a fully humidified atmosphere. The samples were prepared for exposure and immediately treated with radiation at dose rates 1, 5 and 10 Gy 5 min^{-1} from a ^{60}Co source (42.6TBq, AECL, Canada at Korea Atomic Energy Research Institute) at room temperature.

Western blot analysis

Cells were rinsed once with ice-cold PBS and lysed in ice-cold PRO-Prep (iNtRON Biotech, Gyeonggi-do, Korea) lysis buffer. The soluble fraction of the cell lysates was isolated by centrifugation at 13,000xg for 20 min in a microfuge. Supernatants were measured for protein concentration using a detergent-compatible protein assay (Bio-Rad, Hercules, CA, USA), and equal amounts of proteins were separated by 10-15% SDS-PAGE, followed by electrotransfer onto a polyvinylidene difluoride membrane (Millipore, Bedford, MA, USA). The membranes were blocked for 2h with TBS-t (10mM Tris-HCl [pH 7.4], 150mM NaCl and 0.1% Tween-20) containing 5% non-fat milk at room temperature and then incubated with primary antibodies overnight at 4°C. The blots were washed three times for 15 min with TBS-t containing 0.1% Tween 20 and then incubated for 2h with peroxidase-conjugated secondary antibodies (1:4,000) at room temperature. The membranes were washed three more times and

developed using an enhanced chemiluminescence detection system (iNtRON Biotech, Gyeonggi-do, Korea).

Cell cycle analysis

Floating and trypsin-detached cells were collected and washed once with ice-cold PBS, followed by fixing in 70% cold ethanol for 15 min at 4°C. The cells were then washed with ice-cold PBS, resuspended in PBS containing propidium iodide (50 mg/ml), RNase A (100 mg/ml), and 0.1% Triton X-100, and left for 15 min at 37°C under dark condition. To analyze apoptosis, hypodiploid DNA (sub-G1) populations were assayed using a Cytomics FC 500 flow cytometer with Cytometer CXP software (Beckman Coulter, Franklin Lakes, NJ, USA). The results represent the means of triplicate determinations in which a minimum of 10,000 cells were assayed for each determination. Any sub-G1 populations were counted as apoptotic cells.

Detection of senescence

Cellular senescence was measured by staining of the senescence-associated β-galactosidase (SA-β-gal) activity using senescence detection kit (BioVision Research Products, CA, USA) according to the manufacturer's protocol. Cells grown on the coverslip were fixed and then stained with X-gal solution overnight.

Cell-staining with acridine orange

HeLa cells were cultured on cover slips coated with poly-L-lysine (Sigma-Aldrich, USA) and were treated with or without gamma-irradiation. At 24h after IR treatment, cells were then washed twice with PBS. Next, acridine orange was added at final concentration of 1 μg ml^{-1} for a period of 15 min. After washing, the cells were mounted using a Vectashield mounting medium with 4,6-diamidino-2-phenylindole (Vector Laboratories, Burlingame, CA, USA). Fluorescence images were taken using a fluorescence microscope (Olympus, BX50) and SPOT software 5.1 (Diagnostic Instruments, USA). The intensity of red fluorescence is proportional to the degree of acidity and/or the volume of the cellular acidic compartment.

Quantitative measurements of autophagy using flow cytometry

To quantitative measurements of autophagy, we analyzed acidic vesicular organelles (AVOs) by flow cytometry. Stock solution of acridine orange was diluted to a final concentration of 0.1 μg ml^{-1} in serum free media. Cells were washed with 1xPBS, followed by incubation with acridineo range working solution for 15 min in the dark at 37°C. Trypsinized cells were centrifuged and resuspended in PBS. Then the increase in fluorescence was detected by flowcytometry (CytomicsFC500, Beckman Coulter). We analyzed the data with Cytometer CXP software and used the mean fluorescence intensity to quantify responses. The mean fluorescence of 10,000 analyzed cells (corrected for autofluorescence) of each treatment group was taken as a measure of the total acridine orange positive load.

Fluorometric determination of caspase-3 activity

Cells were sonicated in 0.1M Tris-HCl [pH 7.5] for three 2-s bursts. After centrifugation at 13,000xg for 20 min, the supernatants were measured for protein concentration using a detergent compatible protein assay (Bio-Rad), and caspase-3 activity was measured with an caspase-3/CPP32 colorimetric assay kit (BioVision, USA) according to the manufacturer's protocol. After incubating 50 micrograms of proteins with DEVD-pNA substrate, the generation of fluorescent signal (absorbance at 405nm), indicative of caspase-3 activity, was measured by using an automated spectrophotometer. Three independent experiments were performed to determine standard deviation.

3. Results

Activation of p53 in the DNA damage responses

The cellular levels of several proteins related to the cell cycle and apoptosis were analyzed in order to characterize the IR-induced cellular responses. The expression of

p53 protein in HeLa cells was radiation dose and time dependent (Figure 3-1). At 24h post-irradiation, chk1 protein levels were up-regulated according to p53 expression. However, chk1 protein levels were down-regulated as a consequence of p53 expression status by stress signals at 72h post-irradiation. p53 death signals lead to down-regulaton of p21, which might precede caspase activation. At 24h after irradiation, IR-induced DNA damage activates "p53→p21 pathway" leading to elevated p53 and chk1 and cell cycle arrest, thereby allowing time for DNA repair. These results indicated that p53 and p21 were required to block apoptosis and induce autophagy in HeLa cells at 24h post-irradiation.

Immunoblotting demonstrated cleavage of caspase-3, 7 and cleavage of the caspase substrates poly (ADP-ribose) polymerase (PARP) to promote apoptotic pathway at 72h after treatment with gamma-rays. HeLa cells 24h post treatment did not show drastic increase in apoptosis-related proteins.

p53 positively or negatively regulates apoptosis in response to ionizing radiation

For quantitative measurements of apoptosis, cell cycle analysis was conducted. As shown in figure 3-2, accumulation in G1 phase 24h after treatment of HeLa with IR was observed. Cells were arrested in G1 accompanied by up-regulation of p21. G1 arrest is known to be involved in cell survival, thus, the activation of p21 results in resistance of cells to apoptosis [3-2, 3-3]. Previously, it was proposed that low levels of p53 induce cell cycle arrest, whereas high levels of p53 induce apoptosis [3-13]. Following exposure to IR, low levels of p53 might be a negative regulator for apoptosis and inducer for autophagy at the same time. On the other hand, an increase (approximately 12.5%) in sub-G1 population at 72h was observed (Figure 3-2C). High levels of p53 positively regulated apoptotic pathway in HeLa cells 72h after 10 Gy irradiation.

IR-induced cellular responses were triggered with differing p53 status. At the molecular level, DNA damage-induced senescence in human cells is characterized by p53 activation and subsequent accumulation of p21, which leads to growth arrest

[3-17]. In this study, senescence was evaluated as an alternative mechanism of p53-mediated cellular response by IR. The induction of cellular senescence as measured by staining of the senescence-associated β-galactosidase (SA-β-gal) activity was not detected at the indicated incubation time (Figure 3-3), suggesting that p53 and p21 were not essential regulators of stress-induced senescence under our experimental conditions.

p53 promoted autophagy by regulation of LC3

Since apoptotic features and cellular senescence were not shown in HeLa cells at 24h post-irradiation, it was of interest to understand underlying mechanism for survival, autophagy. As a marker of autophagy, the volume of the cellular acidic compartment was visualized by acridine orange staining. Acridine orange-positive cells with higher bright red fluorescence were frequently detected in HeLa cells 24h after 10 Gy irradiation compared to sham control (Figure 3-4A). However, cells at 72h exposure to IR showed no difference (data not shown). To determine whether IR induce autophagy and examine the role of p53 as a cell survival regulator in autophagy, the outcome of autophagy inhibition was determined using 3-methyladenine (3-MA), an autophagy-specific inhibitor (Figure 3-4B). Following 3-MA pretreatment, IR-induced autophagy measured by acridine orange staining was found to be reduced (a 20% reduction).

LC3-I is present in the cytoplasm, and LC3-II, which is formed during autophagy, is present in the autophagosome. During the initiation of autophagy, LC3-I is converted to LC3-II. Thus, LC3 is a marker of autophagosome formation and detecting LC3 is a reliable method for monitoring autophagy. Autophagosome-incorporated LC3-II protein expression increased after 24h irradiation compared to control. Significant change in LC3-II protein was not observed at 72h (data not shown), and the conversion of LC3-I to II was reduced following 3-MA pretreatment (Figure 4, C). These results imply that the expression of p21 by a p53-dependent mechanism is required to develop autophagic properties after DNA damage.

Caspases are not required for autophagic cell death

Next, testing was conducted to determine if the apoptotic cell death observed after p53 induction was dependent on caspase activity. Caspase-3, effector caspase, cleaves various cellular death substrates involved in the regulation and excecution of apoptosis [3-6]. Caspase-3 activity leading to cleavage of DEVD was 2.6-fold higher in HeLa cells obtained at 72h after irradiation than cells at 24h (Figure 3-5A). To confirm this increased activity was induced by p53-mediated apoptosis, broad-spectrum caspase inhibitor benzyloxycarbonyl-Val-Ala-Asp-fluoromethyl ketone (z-VAD-fmk) was added at 10 ug/ml working concentration to sham or irradiated cells. Z-VAD-fmk completely blocked caspase-3 activity. However, the caspase inhibitor did not block caspase-3 activity in cells obtained at 24h post-irradiation, which undergo autophagy. Thus, caspase activaton is not required in autophagy and p53 induce autophagy independent of caspase activation. Z-VAD-fmk treated cells underwent less apoptosis than those 10 Gy irradiated (Figure 3-5B). Cleaved PARP expression induced by apoptotic cell death was reduced by z-VAD-fmk treatment (Figure 3-5C).

4. Discussion

Extensive research has been directed towards the role of p53 as a key regulator in DNA damage surveillance network [3-2, 3-3]. The impetus behind most of these studies has been the model proposed over a decade ago, suggesting that the principal role of the p53 pathway in determining cell fate following genotoxic stress is to either promote survival by activating cell cycle checkpoints, or induce apoptotic cell death [3-18, 3-19].

It is known that p53 responds to DNA damage in various modes, depending on cell and stress types. The level of p53 protein accumulation in response to IR primarily results from the intensity of DNA damage. Apoptosis occurs in response to a high dose of IR when the damage is irreparable, in order to eliminate the damaged cells [3-1~3-3]. The dose of IR predominantly contributes to the outcomes of cell fate, either

survival or death. Herein, our results proposed that IR-induced p53 status could determine cell fate. The p53 protein expression levels in HeLa cells were increased gradually with incubation time after IR treatment. Cells showing distinct features characterized by autophagy (survival) or apoptosis (death) were evaluated at 24h and 72h, respectively.

The “arrester” p53 mediate early checkpoints through p21, and the “killer” p53 mediate apoptosis through caspase-3 [3-18, 3-19]. In this study, HeLa cells were used to characterize the influence of p53 status on cell fate, suggesting a role of p53 in two fundamentally important cell biological pathways: autophagy and apoptosis. Autophagy induction and apoptotic shift may be mediated by p53 activation. Apoptotic cell death was accompanied by caspase activation as well as by cleavage of caspase substrates [3-6]. Proteins related to cell cycle and apoptosis were checked in figure 1. The increased level of p53 was radiation dose and time dependent. Results in this study showed chk1 and p21 cooperate to prevent apoptosis and function in the induction of autophagy under low levels of p53 at 24h post-irradiation. On the other hand, high levels of p53 promoted down-stream proteins related to cell death activated by caspase cascade.

As well known, IR not only makes DNA damage but also arrests cells to G1/S or G2/M phase depending on distinct cell lines [3-20]. In this study, accumulation in G1 phase at 24h after treatment of HeLa with IR was observed (Figure 3-2B). Cells were arrested in G1 phase accompanied by up-regulation of p21. p21 has an ability to influence cell cycle progression as well as anti-apoptotic property inhibiting the activity of proteins directly involved in the induction of apoptosis, including caspase-3 [3-3~3-5]. The activation of p21 induced by p53 at 24h following irradiation resulted in resistance of HeLa cells to apoptosis. In contrast, apoptotic cell population was increased as a consequence of p53 expression status by stress signals 72h post-irradiation (Figure 3-2C).

In addition to cell cycle arrest and apoptosis, numerous studies have identified senescence as an alternative mechanism of p53-mediated cellular responses by IR. Another important role of p21 in the p53 pathway is to switch on the permanent

growth arrest [3-10, 3-21]. Therefore, experiments were conducted to examine whether HeLa cells undergo p53-dependent cellular senescence at the indicated incubation time. However, senescence of either cells at 24h or 72h post-irradiation was not shown (Figure 3). These data demonstrate that p53 and p21 were not central mediator of senescence in response to γ-irradiation under our experimental condition.

Autophagy is frequently activated in tumor cells following anticancer therapies such as drug treatment and γ-irradiation [3-22]. Increased autophagy, the hallmark of programmed cell death type II, is thought to lead to cell death via destruction of the cytoplasm. Still, the lysosomal compartment has been linked to cellular defense mechanisms [3-23]. The pro-survival function of autophagy has been demonstrated at the cellular level [3-24]. At the present time, we are gaining much insight regarding the roles of p53 in autophagy. Our results suggest that p53 promoted autophagy by regulation of LC3 and accumulation of acidic vesicular organelles (AVOs) after irradiation (Figure 3-4). IR-induced p53 activation resulted in cytoprotective autophagy under this condition.

No obvious differences were observed in HeLa cells at 72h post-irradiation, with respect to either senescence or autophagy. To elucidate the role of p53 in IR-induced caspase-3 activation and apoptosis, the outcome of apoptosis inhibition was evaluated. p53 signaling positively regulated apoptosis in response to DNA damage at 72h post-irradiation. Caspase-3 activity as measured by caspase-3 colorimetric assay kit was increased by 2.6-fold compared to sham control. As expected, z-VAD-fmk, pan-caspase inhibitor, completely blocked IR-induced caspase-3 activation and cell death (Figure 3-5 A, B). Caspase-3 functions as effector or executioner, cleaving various substrates including PARP [3-5]. Protein levels of cleaved PARP were checked as a marker for apoptotic cell death. The death resulting from radiation is now, to a considerable degree, understood as radiosensitivity. Our understanding of the IR-induced cellular responses controlled by the p53 suggests a role of autophagy in the protective signaling pathways that enable tumor cells to avoid apoptosis. Without autophagy, genome damage caused by metabolic stress is mostly unhindered [3-25]. Our findings point out the significance of p53 in determining the radiosensntivity of HeLa cells by

inhibiting autophagy and activating apoptosis. Further studies on p53 functioning at the switch from reversible arrest to triggering apoptosis may offer a greater understanding of radioresistance and radiosensitivity.

It has been reported that autophagy induced by IR may prevent cells from undergoing apoptosis, implying an interlink modulation between autophagy and apoptosis [3-26]. The rate of apoptosis and autophagy was determined with different p53 status after IR treatment of HeLa cells in this study. The cross-talk between autophagy, a pathway that functions primarily in cell survival, and apoptosis, a pathway that invariably leads to cell death, is complex. The cellular levels of p53 determine its biological function. In previous studies, the function of hypo- and hyper-physiological levels of p53 was investigated mostly under the conditions induced by artificial modulation of p53 expression [3-14~3-16]. This study was focused on cellular responses induced by physiological levels of p53. It is of crucial importance to evaluate biological effect by IR-induced p53 level for understanding cancer therapy taking radioresistance and radiosensitivity into consideration. Our research on IR-induced cellular responses may provide new information about fate decision between the processes of apoptosis and autophagy.

5. Conclusions

It has been shown in several cell types that p53 protein levels are correlated with cell fate decisions. However, those cellular responses were induced by inhibition or overexpression of p53. Cellular responses induced by artificial regulations of p53 protein levels showed critical features representing the function of p53, but it was far from the biological responses inside the cells. This study was conducted to identify whether physiological levels of p53 induced by IR mediate cell's fate. The rate of apoptosis and autophagy was variable with different p53 status after IR treatment. The influence of p53 status on cell fate suggests a role of p53 in two fundamentally important cell biological pathways: autophagy and apoptosis.

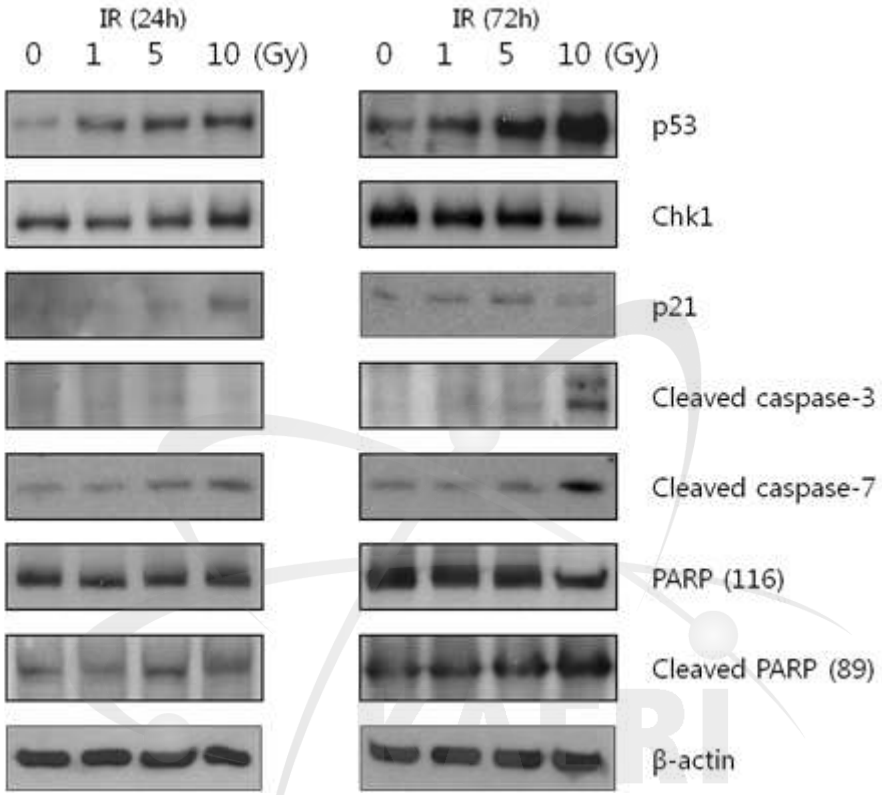

Fig. 3-1. p53 activates p21 but not proapoptotic targets at 24 h post-irradiation. Western blot analysis of HeLa cells. HeLa cells were isolated and analyzed for the expression of proteins related to cell cycle arrest and apoptosis at the indicated incubation time. β-actin was used as a loading control.

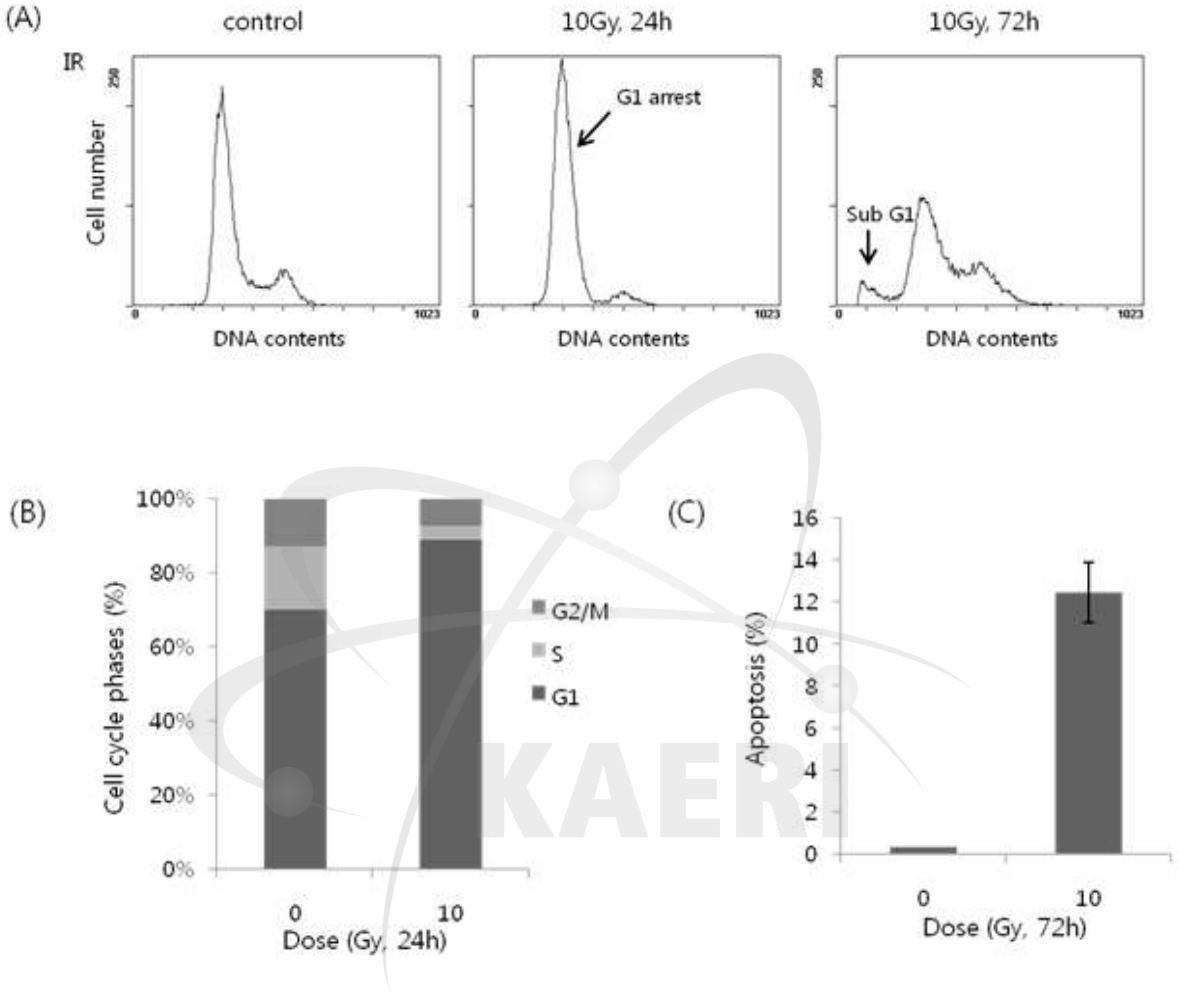

Fig. 3-2. The induction of p21 by p53 influences cell cycle distribution. (A) Repregentitive histograms analyzed by flow cytometry showing G1 arrest 24h post treatment and apoptotic sub G1 fraction at 72h. (B) Cell cycle distribution at 24h post-irradiation. (C) Percentage of apoptosis in HeLa cells 72h post treatment. Any sub-G1 populations were counted as apoptotic cells.

Fig. 3-3. HeLa cells show no evidence of p53-dependent cellular senescence. Images of Senescence Associated β-galactosidase staining of HeLa cells.

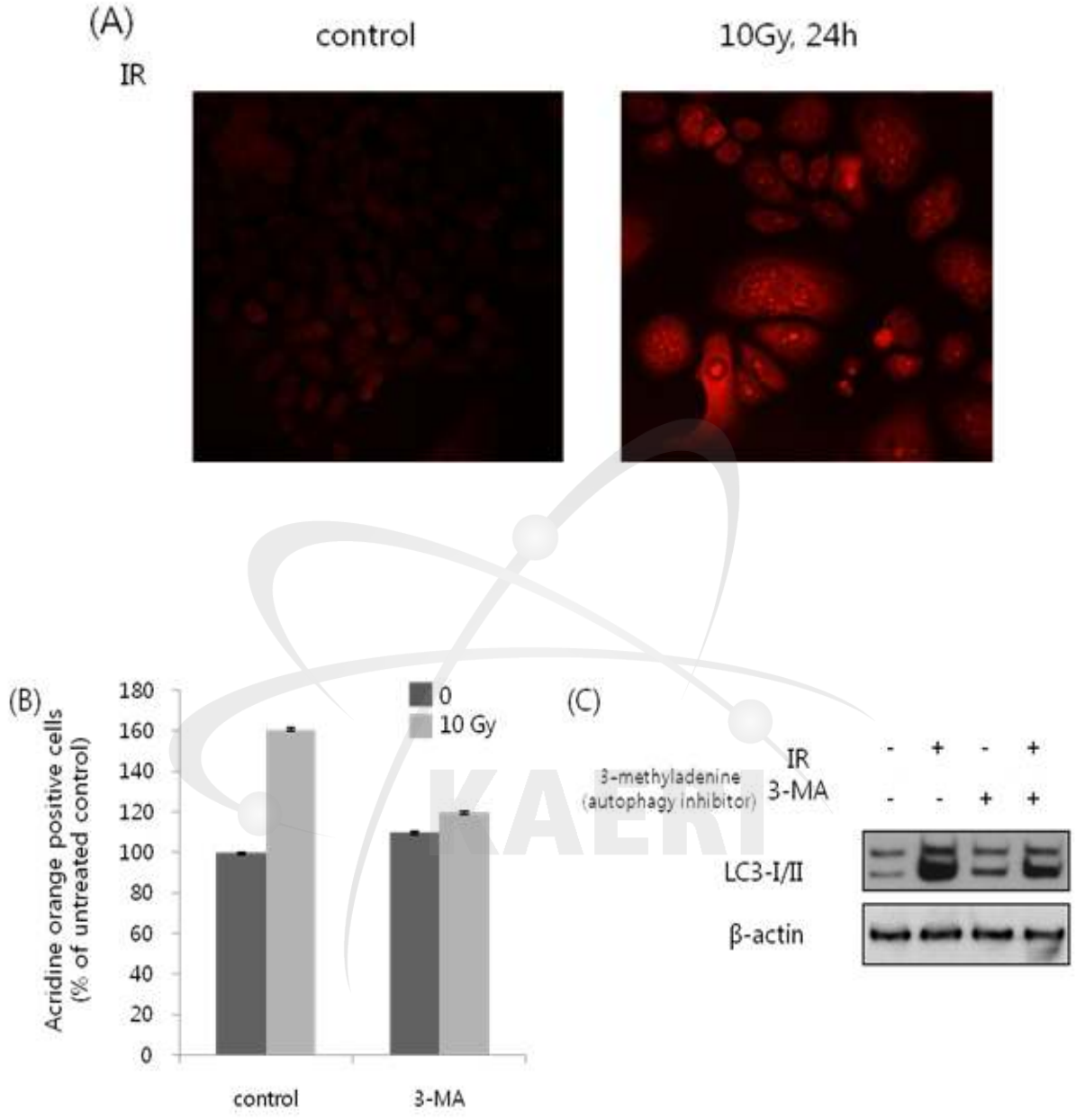

Fig. 3-4. Low levels of p53 trigger autophagy. (A) Detection of radiation-induced appearance of autophagic organelles by vital staining with lysosomotropic agents, acridine orange. (B and C) Effects of inhibitors for autophagy, 3-MA, on acridine orange positive (+) cells and the conversion of LC3-I to LC3-II, respectively.

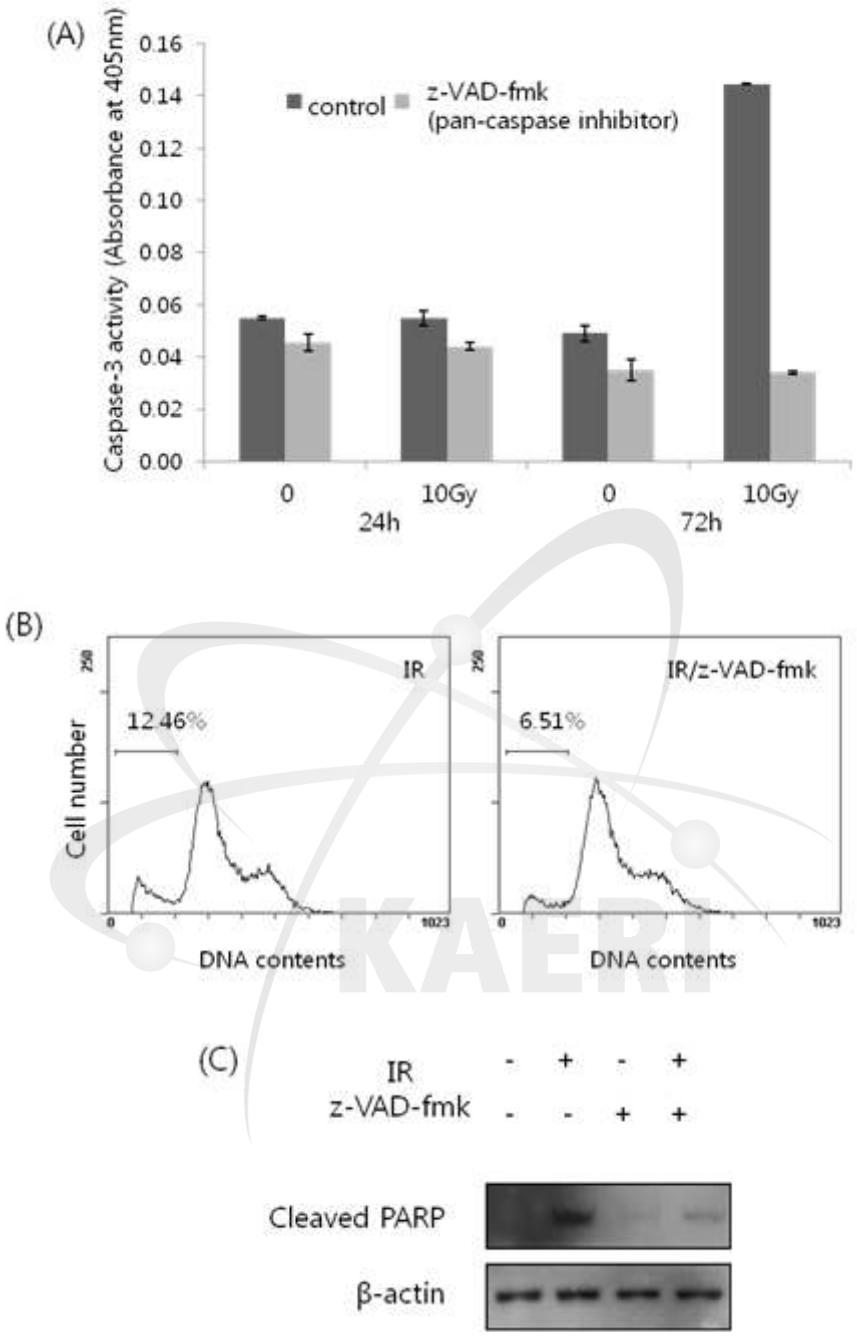

Fig. 3-5. High levels of p53 trigger apoptosis. (A) Caspase-3 activity as measured by caspase-3 colorimetric assay kit at the indicated time incubation. Z-VAD-fmk ompletely blocked caspase-3 activity at 72h post-irradiation. (B) Apoptosis (%) was abrogated by z-VAD-fmk. (C) Cleaved PARP expression induced by apoptotic cell death was reduced by z-VAD-fmk treatment.

제4절 방사선 노출에 따른 세포생존율 측정 검증

Evaluation of cell viability after irradiation with different assays

1. Introduction

Radiation therapy is a powerful tool for cancer treatment [4-1. 4-2]. Human hepatocellular carcinoma (HCC) is a liver cancer and the fifth most common cancer in the world [4-3]. Human hepatoma (HepG2) cells are used as a HCC model in vitro [4-4]. Radiation can lead to cell death [4-5. 4-6]. In cancer treatment, cell viability is a basic and important point for predicting radio-sensitivity in human cancer [4-7, 4-8]. Radiation-induced cell viability is also a significant work for biological research such as DNA repair, cell cycle, and apoptosis [4-9, 4-10]. To date, the Clonogenic assay has been extensively used for measurement of cell viability in radiation study [5-11~4-16]. However, the conventional Clonogenic assay remains unsatisfactory. It is a colony formation assay which is labor-intensive and time-consuming (incubation time; 1-2weeks). Therefore it is necessary to look over a rapid and easy assay for determination of radiation-induced cell viability.

Both MTT and Trypan blue assay are a routine and convenient method for determination of cell viability [4-17, 4-18]. The MTT assay is a colorimetric assay, which is based on the cleavage of the yellow tetrazolium salt MTT to purple formazan crystals by only viable cell. Usually, it is performed in 96 well microplates and measured the absorbance using the micro-plates reader. The Trypan blue assay is a dye exclusion staining assay, which is based on uptake of trypan blue dye by dead cells due to loss of their membrane integrity, so the dead cells appear darker than the viable cells. It is measured by using a hematocytometer and a microscope or cell counting instruments. The aim of this study was to compare the MTT and Trypan blue assays for radiation-induced cell viability in cultured HepG2 cells on 96 well plates. Also, we determined the relationship between cell viability and cell density after irradiation and confirmed the radiation-induced cell viability according to cell density by using the Clonogenic assay.

2. Materials and Methods

Materials

Trypan blue reagent, Dulbecco's modified Eagle's medium (DMEM), fetal bovine serum (FBS), Penicillin, and other cell culture reagents were purchased from Gibco BRL(FRANCE). Tetrazolium (MTT) was purchased from Roche (Mannheim, Germany). Crystal violet was purchased from YD diagnostics (Gyeonggi, Korea). All other reagents were obtained from analytic grade.

Cell Culture

HepG2 were purchased from American Type Culture Collection (ATCC, USA). The cells were cultured in DMEM supplemented with 10% fetal bovine serum (Invitrogen, Carlsbad, CA) and penicillin (100 U/ml) at 37 ℃ in 5% CO_2. The cells were harvested following trypsinization (0.025% trypsin and 0.02% EDTA) and washed twice with phosphate buffered saline (PBS). When the cell density reached approximately 80% confluence, the cells were subcultured. The cell viability was determined using the Trypan blue, MTT, and Clonogenic assay. Cells (1000, 3000, 5000, 10000 cells/well) were seeded in 96-wllplates, incubated overnight, and irradiated with 1-100 Gy. Then, the cells were incubated for 1, 2 and 3 days, respectively. These samples were used for different cell viability assays (MTT, Trypan blue, and Clonogenic assay)

.

Typan blue assay

The Trypan blue assay was measured by previously described [4-17]. One to three days afte rirradiation, cells were detached by trypsinization and the number of viable cells was counted using a Trypan blue stain reagent. The viability of the control (untreated cells) was regarded as 100%.

MTT assay

The Trypan blue assay was measured by previously described [4-18]. One to three

days afte rirradiation, cells were treated with MTT reagent. The absorbance at 570 nm was measured using a microplate reader (MutiskanEX, ThermoLabsystems). The viability of the control (untreated cells) was regarded as 100%.

Clonogenic assay

The Clonogenic assay assay was measured by previously described [4-19] . Afte rirradiation, cells were incubated for 1, 2, and 3 days, respectively. Then, cells were tryypsinized, counted, and seeded in triplicated in 100-mm dishes (100 and 500 cells per dish) and incubated for 14 days to allow for colony growth. After 14 days, colonies are fixed with 70% ethanol, stained with crystalviolet (0.3%) and counted using a counter. The survival(%) was calculated as (number of colonies/number of cells plated) / (number of colonies for corresponding sham-irradiated control/number of cells plated) x 100.

Irradiation

Cells were irradiated with gamma radiation from a ^{60}Co gamma irradiator (7.4 PBq capacity; AECL, Canada) at Korea Atomic Energy Research Institute.

3. Results

Radiation-induced cell viability in HepG2 cells using Trypan blue and MTT assay

To compare the cell viability effect of radiation on HepG2 cells, we used MTT and Trypan blue assays (Fig. 4-1). Cell viability was determined over 3 days using the two assays. When cells were seeded in 96-well plates at an initial cell density of 1 x 10^4 cells/well, the viability was decreased in a dose-dependent manner as assessed by the Trypan blue assay (Fig. 4-1A). The cell viability was about 50% for 3 days after 5 Gy irradiation in the Trypan blue assay. However, the viability value of the MTT assay displayed no significant changes (Fig. 4-1B). Even after irradiation of upto 100

Gy, the decrease of viability was not observed.

To study why the MTT assay was not effective to cell viability, we examined the relationship between cell viability and cell density (1 x 10^3, 3x10^3, 5x10^3 and 1x10^4 cells/well) by using the MTT assay (Fig. 4-2A). When the cell density was 1x10^3 cells/well, the viability was decreased by about 50% for 3 days after 5 Gy irradiation. In the cell density of 1x10^3cells/well, the cell viability measured by the MTT assay was decreased in a dose-and time-dependent manner (Fig. 4-2B). Also, we tested the Tyrpan blue assay at the same cell density. In the Trypan blue assay, the viability was measured as a dose-and time-dependent pattern when the cell density was 1x10^3cells/well (data not shown in the report).

Radiation-induced cell survival in HepG2 cells using Clonogenic assay

To confirm that radiation induces cell death in HepG2 cells, we performed the Clongenic assay. When the cell density was 1 x 10^4 cells/well, radiation resulted in a decrease of cell survival(%) in a dose-dependent manner (Fig. 4-3). After 5 Gy irradiation, there was about 50% of cell survival. However, there was no colony formation at 50 and 100 Gy. Regardless of the initial cell density (1x10^3 ~ 1x10^4 cells/well) and the incubation time (1-3days) after irradiation, 5 Gy radiation induced about 50% of cell death (data not shown in the report).

4. Discussion

Radiation has extensively been used as a tool of cancer treatment [4-1, 4-2]. The exposure of cells to radiation can lead to cell death such as apoptosis or necrosis[20]. It was confirmed that HepG2 cells after irradiation resulted in a dose-dependent viability loss by using the MTT and Trypan blue assays in this research.

There are various assays for cell viability such as the Trypan blue [4-17], MTT [4-18], XTT [4-21] and Clonogenic assay [4-19]. Among these assays, the Clonogenic assay has exclusively been used for the determination of cell survival in radiation

study. However, there has been few reports about the evaluation of MTT and Trypan blue assay on HepG2 cell viability afte rirradiation. In this study, it was found that the MTT, Trypan blue and Clonogenic assay gave similar results for radiation-induced cell viability under different condition (cell density and assay time). After irradiation, the incubation time was 3 days for the Trypan blue and MTT assays whereas 14 days for the Clonogenic assay. Notably, the MTT assay of HepG2 cells was not efficient at a cell density of $1x10^4$cells/well. In the MTT assay, HepG2 cells were usually seeded at a cell density of $>1x10^4$cells/well on 96 well-plates in cell biology experiments [4-22~4-25]. In this study, it was found that optimal cell density for the effective MTT assay in HepG2 cells was a $1x10^3$cells/well on 96 well-plates in order to measure cell viability loss caused by exposure to radiation. This result indicated that it is necessary to consider the optimal cell density for radiation-induced cell viability test using the MTT assay.

In conclusions, radiation-induced cell viability of HepG2 cells was investigated as follow; 1) In both the MTT and Trypan blue assays, the cell viability was decreased in a dose-dependent manner and 5 Gy irradiation induced 50% of cell viability loss. 2) An incubation time (3 days) for both assays was shorter than that (14 days) of the Clonogenic assay. 3) For the effective MTT assay on 96-well plates, an optimal cell density was 1×10^3cells/well.

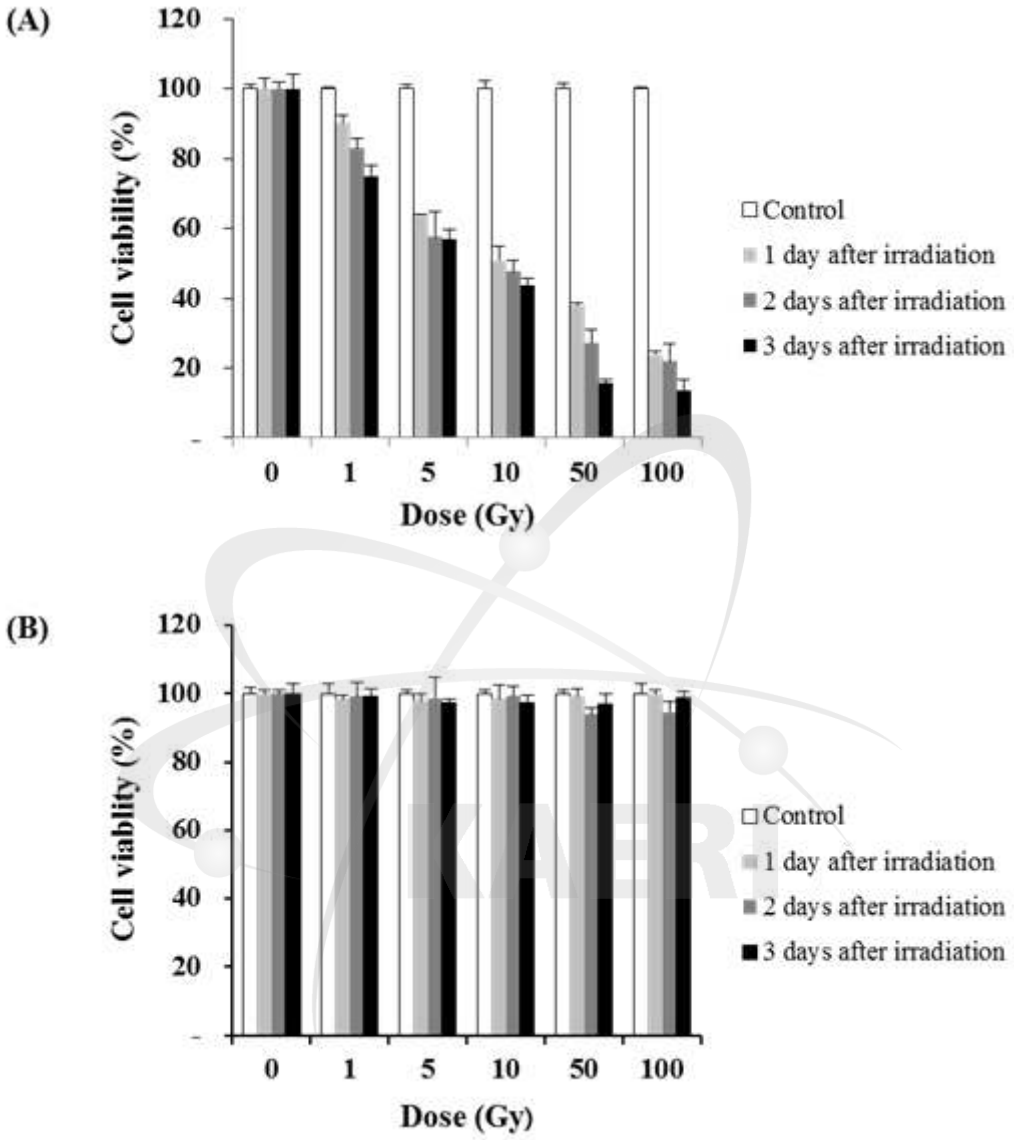

Fig. 4-1. Radiation-induced cell viability on HepG2 cell by using Trypan blue assay (A) and MTT assay (B). Cells were plated on 96 well plates (1 x 10^4cells/well) for 1 day and then irradiated with 0- 100 Gy. After incubation for 1, 2 and 3 days, cell viability was measured by both assays, respectively. Data are mean±SD of triplicate determinations.

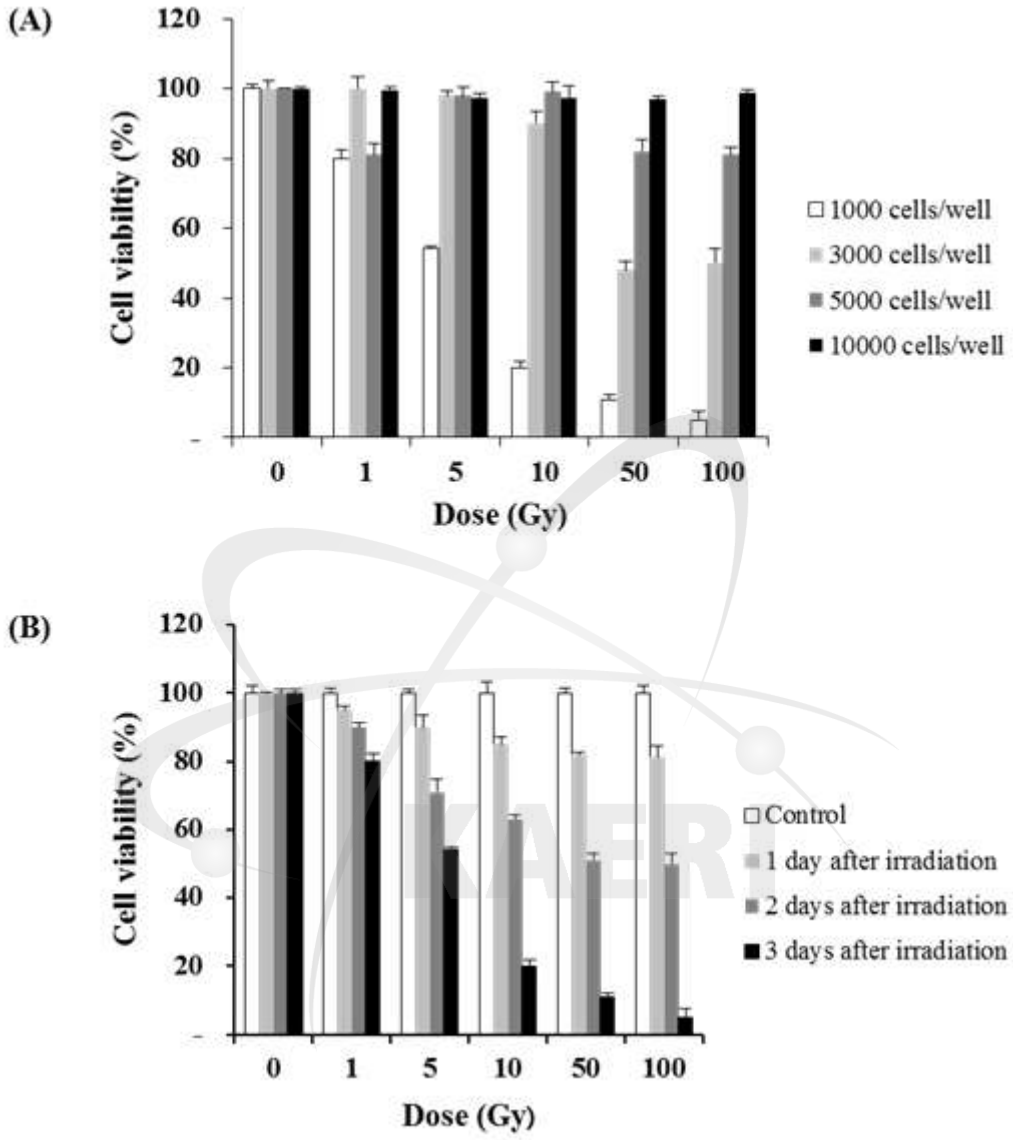

Fig. 4-2. The relationship between cell viability and cell density (1 x 10^3, 3x10^3, 5x10^3 and 1x10^4 cells/well) 3 days after irradiation(A) and time-course of cell viability at cell density (1x10^3cells/well) one to three days after irradiation(B). Cells were plated on 96 well plates (indicated cell density) for 1 day and then irradiated with 0- 100Gy. After incubation for indicated day, cell viability was measured by the MTT assay, respectively. Data are mean±SD of triplicate determinations.

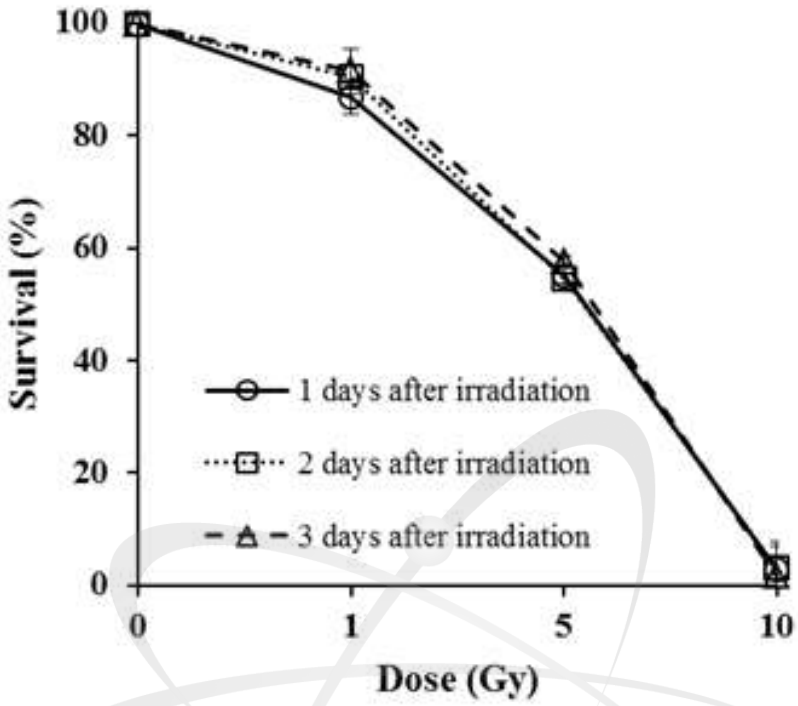

Fig. 4-3. Radiation-induced cell survival on HepG2 cell. Cells were plated on 96 well plates (1 x 10^4 cells/well) for 1 day and then irradiated with 0- 100Gy. After incubation for 1, 2 and 3 days, the Clonogneic assay was carried out. Data are mean±SD of triplicate determinations.

제5절 커큐민의 방사선 방어효과

Radiomodification of curcumin - radioprotective effects

1. Introduction

Ionization radiation (IR) has become a useful resource in human life. It has been used in a wide range of industry including electricity, medicine, food, agriculture, and environment [5-1, 5-2]. The use of radiation is also associated with undesirable radiation exposure or accident threating human health [5-3]. It is well known that IR can penetrate living tissue or cells through the transfer of radiation energy to biological materials such as DNA, RNA, lipid and protein [5-4]. The absorbed energy of IR can cause DNA damage and result in cell dysfunction and even cell death [5-5]. Hence, the radioprotection research is an area of great importance. Amifostine (WR-2721), thiol synthetic compound, has been reported to be the most effective radioprotector studied so far [5-6, 5-7]. However, this compound has adverse effects such as toxicity. In this view, polyphenol derived from dietary plants is of considerable interest due to its safety and antioxidant activity [5-8, 5-9]. Turmeric (Curcuma longa) has been consumed as food and medicine for a long time [5-10]. Curcumin (structure shown in Fig. 5-1) is a yellow pigment and major polyphenol found in turmeric [5-11]. It has been reported to possess many biological effects such as antioxidant, antiinflammatory, and anticancer properties [5-12~5-14]. Curcumin has also been known to protect against IR-induced cell damage in vitro and in vivo study [5-15, 5-16]. However, there is no report on the radioprotective effect of curcumin on DNA damage in human hepatoma (HepG2) cell line, a good cell model for studying cytoprotective and antigenotoxic effects of compounds [5-17, 5-18].

Cytotoxicity and genotoxicity assays have been used to detect cellular response to IR [5-19]. The Clonogenic survival assay (colony counting) is a conventional tool to determine cytotoxicity in radiation cell biology [5-20]. The Comet assay (single cell gel electrophoresis) is a powerful technique for assessing DNA damage and is used to study genotoxicity [5-21]. The main lesions by the interaction between radiation and

DNA are single and double strand breaks, DNA-DNA and DNA-protein cross-links, alkali labile sites and damage to pyrimidine and purine bases [5-22, 5-23]. All these types of DNA damage can be detected by the alkaline version of the Comet assay [5-24, 5-25]. In this study, the radioprotective effects of curcumin against IR-induced cytotoxicity and genotoxicity in HepG2 cells were investigated by using two assays.

2. Materials and Methods

Materials

Curcumin and dimethyl sulfoxide (DMSO) were obtained from Sigma Aldrich (St. Lousi, MO, USA). Dulbecco's modified Eagle's medium (DMEM), fetal bovine serum (FBS), penicillin, and other cell culture reagents were purchased from Gibco BRL (Grand Island, NY, FRANCE). Fetal bovine serum was obtained from Introgen (Carlsbad, CA, USA). Crystal violet was purchased from YD diagnostics (Gyeonggi, Korea). All other reagents were obtained from analytic grade.

Cell Culture and Treatment

HepG2 cells were purchased from American Type Culture Collection (ATCC, USA). Cells were maintained in a DMEM medium supplemented with 10% FBS and penicillin (100 U/ml). Cells were kept in a humidified atmosphere containing 5% CO2 at 37℃. Cells (1 x 106 cells/dish) were plated in 10-cm plastic Petri dishes (10 ml of media) and incubated overnight. The cells were pretreated with or without 5 μM curcumin in FBS-free DMEM for 2 h and then irradiated with 0, 1, 5 and 10 Gy. Curcumin was dissolved in 100% DMSO (w/v) to obtain a stock solution of 10 mM. The working solution was diluted with sterile distilled water so that the final concentration of DMSO in the culture medium was not more than 0.1% (v/v). 0.1% DMSO was used as control. In our experiments for radioprotective effect of curcumin, HepG2 cells were categorized into 3 groups as follows. Control group: non-irradiated cells (sham control), IR alone group: irradiated cells with 1, 5, and 10 Gy, Cur + IR group:

curcumin-pretreated cells in combination with irradiation.

MTT assay

MTT assay was performed according to the manufacturer's instruction (Roche, Germany). Briefly, HepG2 cells were plated at a density of 1 x 104 cells/well in 96 well-plates for overnight. Cells were then treated with different concentrations (1, 10, 25, 50, 100 μM) of curcumin in FBS-free DMEM for 24 h. After the incubation period, 10 μL of MTT (5 mg/mL) was added to each well and incubation was allowed to continue for further 4 h. Finally, 100 μL of solubilization solution (10% SDS in 0.01 M HCl) was added to each well and the plate was stranded overnight in the incubator. The plate was read using a microplate reader (BIO-RAD, USA) at a wavelength of 570 nm.

Clonogenic survival assay

Clonogenic survival assay was performed as previously described [5-20]. One day after irradiation, cells were harvested with trypsin, counted and plated in 10-cm dishes at the appropriate cell number (100 and 500 cells / dish). Then, cells were incubated for 14 days, fixed with 75% ethanol, and stained with 0.3% crystal violet. And colonies were counted to calculate the survival (%). The survival (%) was calculated as (number of colonies/number of cells plated)/(number of colonies for corresponding sham-irradiated control/number of cells plated) x 100.

Comet assay

Comet assay was performed as previously described [5-21]. Following irradiation, the cells were immediately isolated with trypsinization and examined for DNA damage using the alkaline Comet assay. The Comet assay was carried out under dark conditions. Cell suspensions (20 μL) mixed with 0.5% low-melting agarose (200 μL) were spreaded to slides pre-coated with 1% normal-melting agarose. The third layer of 0.5% low-melting agarose was added and solidified. After the solidification of gel layer, the slides were immersed in a lysis buffer (2.5 M NaCl, 100 mM EDTA, 10 mM Tris,

1% Triton X-100 and 10% DMSO, pH 10.0) at 4oC for 60 min. After lysis, slides were placed in electrophoresis buffer (0.3 M NaOH, 1 mM EDTA, pH 13) to allow DNA to unwind for 20 min. Subsequently, slides were subjected to electrophoresis (25 V, 3 00 mA, and 25 min) in the same buffer. Slides were neutralized with Tris-HCl buffer, pH 7. 5, and stained with propidium iodide (20 μg/mL) for 10 min. Slides were examined using an image analysis system (Komet 4.0 from Kinetic Imaging Ltd., Liverpool, UK). Comet parameter was expressed as follows. Tail length (TL), Olive tail moment (OTM) = (Tail mean . Head mean) x Tail% DNA/100, Tail length moment (TEM) = Tail length x Tail% DNA/100, Percentage of Tail (%TL) = 100 - Head% DNA.

Irradiation

HepG2 cells were irradiated with gamma radiation from 60Co gamma irradiator (7.4 PBq of capacity; AECL, Canada at Korea Atomic Energy Research Institute). After pretreatment, the cells were irradiated with 0, 1, 5 and 10 Gy.

3. Results

Cytotoxic effects of curcumin on cell viability in HepG2 cells

To examine the cytotoxic effect of curcumin in HepG2 cells, cell viability was measured by MTT assay. HepG2 cells were treated with various concentrations of curcumin (0, 1, 10, 25, 50 and 100 μM) for 24 h. As shown in Fig. 5-2, there was no cytotoxic effect on cell viability at concentrations ranging from 1 to 10 μM curcumin. Therefore, 5 μM curcumin was used for subsequent experiments.

Cytoprotective effect of curcumin on cell survival in HepG2 cells

To determine the protective effect of curcumin against IR-induced cytotoxicity, the Clonogenic survival assay was performed. HepG2 cells were treated with or without 5 μM curcumin for 2 h and then irradiated with 0, 1, 5 and 10 Gy and incubated for 1 d. As shown in Fig. 5-3, there was a significant decrease of cell survival in a

dose-dependent manner in the IR alone group. The value of 50% lethal dose (LD50) was about 5 Gy in HepG2 cells. The percentage of survival of HepG2 cells significantly increased in the curcumin plus IR group as compared to the IR alone group. It indicated that pretreatment of 5 μM curcumin attenuated cell death by induced IR.

Antigenotoxic effect of curcumin on DNA damage in HepG2 cells

To investigate the IR-induced DNA damage in HepG2 cells, the alkaline Comet assay was carried out. DNA damage in HepG2 cells were analyzed after exposure to 0, 1, 5, and 10 Gy and immediately isolated to avoid DNA repair. Comet parameters including percentage of tail DNA (% TD), total extent moment (TEM), olive tail moment (OTM) and tail length (TL) were used for determining DNA damage. As shown in Fig. 5-4, the levels of comet parameters were increased in a dose-dependent manner. It indicated that IR caused a significant increase of DNA damage in HepG2 cells. To evaluate the antigentoxic effect of curcumin against IR-induced DNA damage, HepG2 cells were treated with or without 5 μM curcumin for 2 h, irradiated with 0, 1, 5, and 10 Gy and analyzed by the Comet assay. As shown in the previous Table 5-1, IR increased DNA damage of HepG2 cells in a dose-dependent manner in the IR alone group. After irradiation, the fragmented DNA formed a typical comet tail-like pattern. The higher dose led to a longer DNA tail length and darker DNA intensity, indicating that IR induced genotoxicty in HepG2 cells. In contrast, pretreatment of 5 μM curcumin decreased DNA tail length. At 5 Gy, the level of comet parameters in the IR alone group was 67.9 ± 9.71 (% TD), 9.96 ± 2.53 (TEM), 3.18 ± 0.90 (OTM) and 14.93 ± 1.59 (TL). In contrast, the level of comet parameters in the curcumin plus IR group was 5.86 ± 0.90 (% TD), 0.48 ± 0.38 (TEM), and 0.26 ± 0.12 (OTM), and 8.63 ± 2.60 (TL) (Fig. 5-5). Thus, the level of the curcumin plus IR group was lower than that of the IR alone group in all comet parameters. It indicated that pretreatment of 5 μM curcumin protected against IR-induced DNA damage in HepG2 cells.

4. Discussion

Exposure to IR induces complex cellular responses which are involved in genomic alterations, mutagenesis, and apoptosis [5-26]. DNA is the major target of cellular response to IR. Also, DNA damage response in cells is important for the accurate prediction of human health risks after chronic or acute exposure to IR. Cytotoxicity and genotoxicity are considered as the major events in cellular responses after exposure to IR. It has been demonstrated that cellular DNA damage induced by IR can cause cell death in organisms [5-27]. In this study, it was found that IR induced cytotoxicity and genotoxicity in HepG2 cells as assessed by the Clonogenic survival assay and the Comet assay. Here, HepG2 cells were used as in vitro cell model for evaluation of radiation protection. HepG2 cells are a human hepatic cell line and have been used as a good model to study in vitro xenobiotic metabolism and toxicity due to many characteristics of hepatocytes such as phase I and II enzymes which play important roles in the activation and detoxification of DNA-reactive carcinogens [5-17]. With regard to radioprotectors, many polyphenols derived from dietary plants have been screened for radioprotective effect [5-6]. Among them, curcumin is considered as a good candidate of radioprotector because of its potential protective role in the pathogenesis of multiple diseases and a variety of biological activities [5-11, 5-28]. It has been reported that curcumin could confer radioprotective effect in vitro and in vivo study [5-15, 5-16]. Lee et al. [5-29] have reported that curcumin improved survival after exposure to IR in vivo experiment. In this study, cell survival (%) was used as an indicator of cytotoxicity. Our result showed that IR induced dose-dependent cytotoxicity in HepG2 cell after exposure to IR ranging from 0 to 10 Gy. In contrast, pretreatment of HepG2 cells with 5 μM curcumin for 2 h before exposure to various dose of IR resulted in a significant increase of cell survival when compared with that of the IR alone group. Srinivasan et al. [5-16] reported that pretreatment of curcumin (10 μg/ml) could protect human lymphocytes against γ-radiation induced DNA damage by using micronucleus assay and dicentric aberration assay. Abraham et al. [5-15] reported that oral administration of chlorogenic acid, curcumin and β-carotene could

exert protective effects against γ-radiationinduced chromosomal damage in Swiss albino mice by using a micronucleus assay. However, there has been no report on the protective effect of curcumin against radiation-induced DNA damage in HepG2 cells by using the comet assay. In this study, DNA damage was used as an indicator of genotoxicity. Our result showed that curcumin had an ability to protect cells against IR-induced DNA damage by reducing the increased level of all comet parameters after exposure to IR.

In conclusion, we evaluated the cytoprotective and antigenotoxic effect of curcumin in HepG2 cells after exposure to IR by using the Clonogenic survival assay and the Comet assay. Pretreatment of 5 μM curcumin attenuated IR-induced toxicity, cell death and DNA damage, in HepG2 cells. The results suggest that curcumin could act as a radioprotector.

Table 5-1. Parameters of DNA damage induced by IR in HepG2 cells

Radiation dose (Gy)	%TD	TEM	OTM	TL
0	18.21±12.68	1.94±1.71	0.70±0.21	10.68±2.01
1	53.03±25.84	6.987±4.36	2.44±1.49	12.86±2.90
5	67.90±9.71*	9.96±2.53*	3.18±0.90*	14.93±1.59
10	73.42±2.70*	11.81±4.53*	4.11±0.36*	16.64±1.85*

%TD, Percent of Tail DNA; TL, Tail length; OTM, Olive tail moment; TEM, Tail extent moment.

Data are presented as mean ± S.D. (n=3).

Significantly different from the non-irradiated groups: * $P<0.05$; ** $P<0.01$.

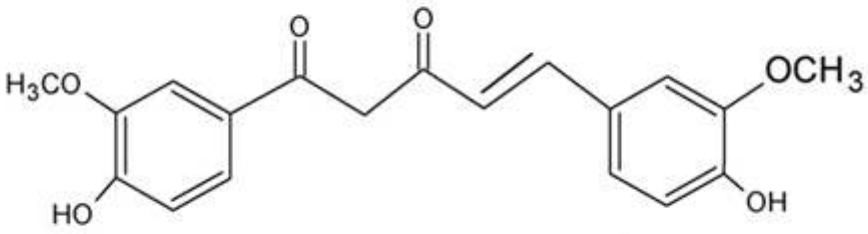

Fig. 5-1. Chemical structure of curcumin.

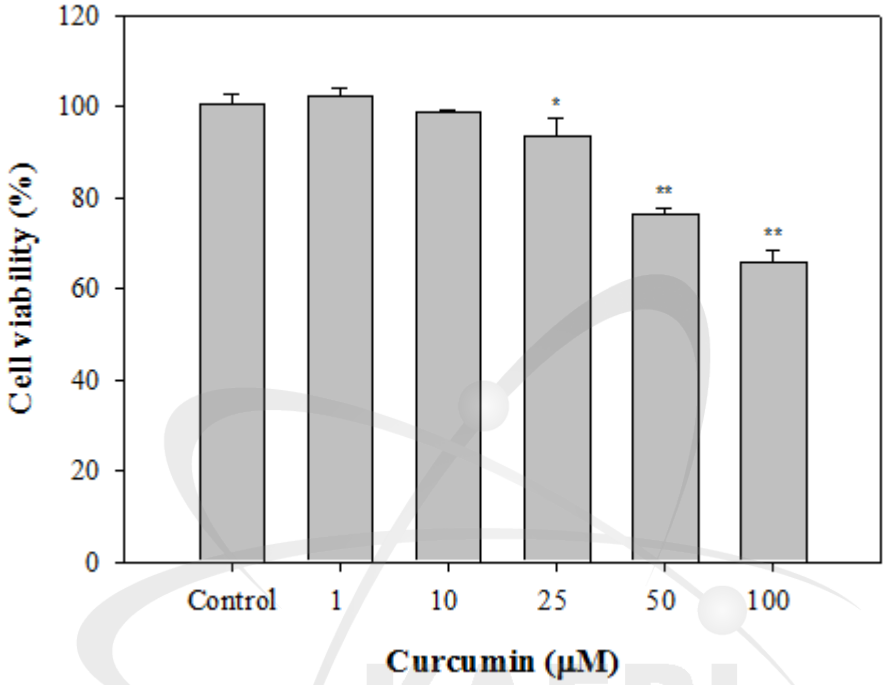

Fig. 5-2. Cytotoxicity of curcumin by using MTT assay. Data are represented as mean ± SD (n=3). (n=3). $*p < 0.05$, $**p < 0.01$ compared with control group.

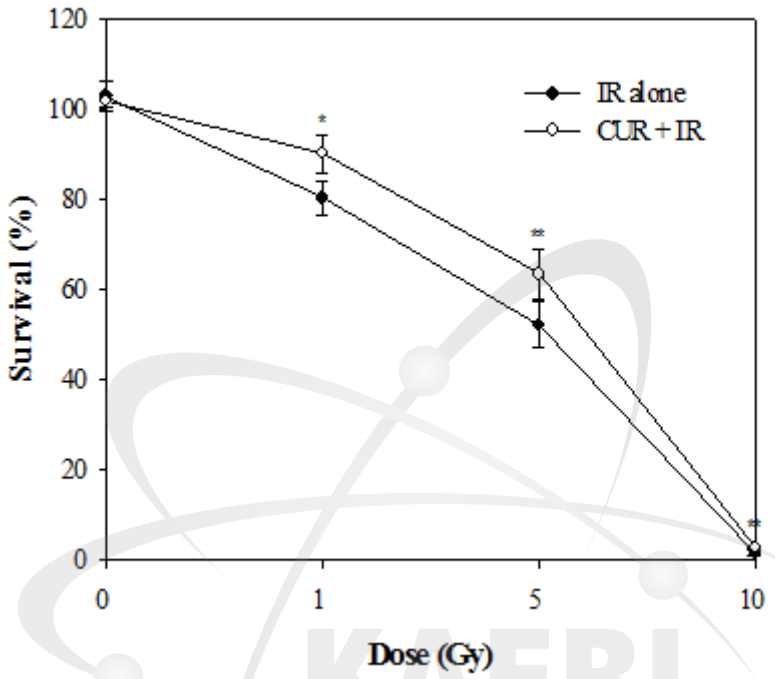

Fig. 5-3. Effect of curcumin against IR-induced cytotoxicity in HepG2 cells as determined by the Clonogenic survival assay. Data are represented as mean ± SD . *(n=3). *p* < 0.05, ***p* < 0.01 compared with control group.

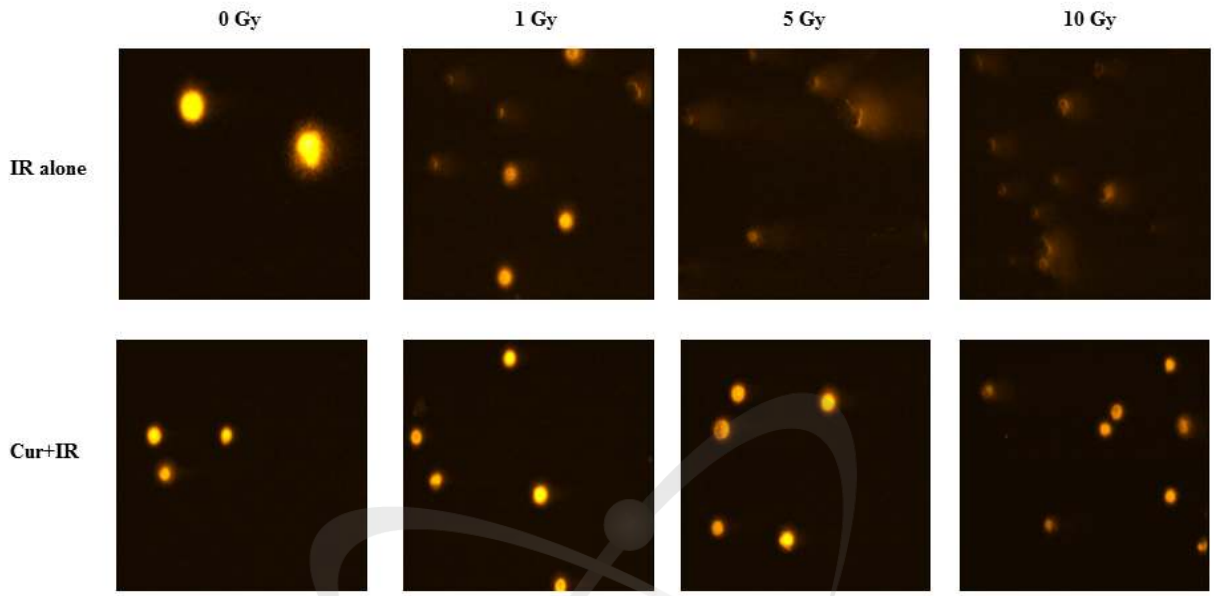

Fig. 5-4. Comet images of the IR alone and curcumin plus IR group in HepG2 cells.

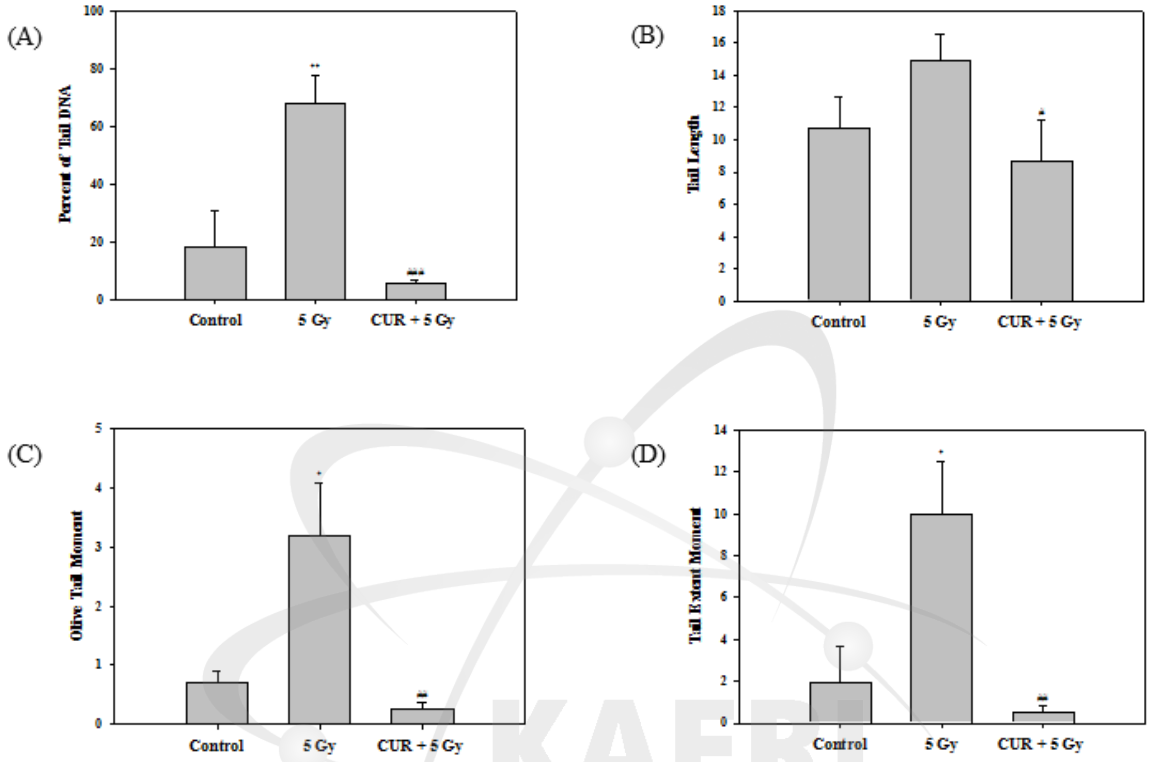

Fig. 5-5. Effect of curcumin against IR-induced genotoxicity in HepG2 cells as measured by the Comet assay. HepG2 cells irradiated with 5 Gy. Data are represented as mean ± SD . *(n=3).* $*p < 0.05$, $**p < 0.01$ compared with control group.

제6절 세포에 대한 고 LET 및 저 LET 방사선의 복합작용

Cell responses to combined action of low and high LET radiations

1. Introduction

The relative biological effectiveness (RBE) of ionizing radiation with a high linear energy transfer (LET) is known to be dependent on the function of genes controlling cell recovery from radiation damage. In particular, for unicellular organisms of various origins, the RBE was greater for cells capable of recovery than for cells with a reduced ability to recover, or completely missing such ability [6-1~6-6]. In other words, RBE is determined both by the probability of primary damage production (physical events) and the ability of a cell to recover from radiation damage (biological events). There seems to be common agreement that high-LET radiation, compared with low-LET radiation, produce a higher proportion of damage that is considered to be irreversible [6-7~6-10]. This is an important case for the recovery from potentially lethal radiation damage observed in irradiated mammalian and yeast cells. More detailed patterns of such recovery at the cellular [6-11~6-13] and molecular [6-14~6-16] levels are well-known for yeast cells. Furthermore, the ability of eukaryotic cells to recover from radiation damage was first discovered in experiments with yeasts [6-17]. If irradiated yeast cells are held in liquid non-nutrient medium at 30℃ before plating onto a growth medium, their survival is increased. This phenomenon is now known as liquid-holding recovery (LHR) [6-18]. The quantitative approach describing the recovery process as a decrease in the effective dose is well-known [6-11] and it was applied for yeast [6-19, 6-20] and mammalian cells [6-21] exposed to ionizing radiation combined with various chemical and physical agents. This approach allows one to determine whether the process of recovery after combined actions is destroyed or damaged itself, or whether the decrease in the rate and extent of recovery is entirely due to an increase in the fraction of irreversible damage. There are very little data on the analysis of radiosensitivity and the ability of cells to recover after repeated exposures, which are often used in practice. For example, Korogodin [6-11] analyzed

radiosensitivity and LHR after repeated exposures of yeast cells only to low-LET radiation. Similar studies have not been conducted with densely ionizing radiation that causes more severe, irreparable damage. The repeated irradiations were shown not to change the radiosensitivity of the cell, but to result in a reduced ability of the cell to recover, which was expressed both in the extent and the rate of recovery [6-11]. These effects may arise either from damage to the recovery process itself, or from the formation of irreversible dam-age that cannot be repaired at all. Both processes may take place at the same time. However, data distinguishing these possibilities are lacking in the literature. The data related to reduction of the ability of cells to recover from sub-lethal radiation damage after repeated irradiations are well-known for cultured mammalian cells. The progressive reduction in the extrapolation number up to complete disappearance of the shoulder in the sigmoid dose response curve is also well-known for high-LET radiation [6-22]. The cellular ability to recover from potentially lethal damage after repeated exposures to low-and high-LET radiation has hardly been studied. Qualitatively, most radiobiological responses of yeast and mammalian cells are similar to each other. For example, survival curves for haploid yeast and mammalian cells are exponential. Conversely, survival curves for diploid yeast and mammalian cells are sigmoid. Therefore, yeast cells are a convenient model for studying the cellular ability to recover from potentially lethal damage after repeated exposures to radiation of different quality. Our investigation has been undertaken to examine these issues in yeast cells. In this study, the liquid-holding recovery will serve as an indicator of the cellular repair activity. Understanding of the underlying mechanism will hopefully lead to a better insight into the relationship between radiation of various quality and cell recovery from potentially lethal radiation damage. Thus, the main goals of this study were (a) to study radiosensitivity and recovery of yeast cells after repeated exposure to low- and high-LET radiation; (b) to answer the question whether or not high-LET radiation affects the recovery process itself, or whether it only produces a higher level of severe and irreversible damage that cannot be repaired at all; (c) to elucidate the RBE of high-LET radiation after repeated irradiation of yeast cells.

2. Material and methods

The yeast *Saccharomyces cerevisiae* (strain XS800, diploid) in the stationary phase of growth was used for these experiments. To attain this phase, cells were incubated before irradiation on a solid nutrient agar during four days. After attaining the stationary phase of growth, the cells were washed with distilled water and a cell suspension of 5×10^7cells/ml was prepared. Cells from the same stock solutions were irradiated with ^{60}Co γ-rays (23 Gy/min) and with ^{239}Pu α-particles (20 Gy/min). The LET of the particles reaching the cell monolayer was estimated to be about 120 keV/μm. Just at this LET value the maximum in RBE-LET relationship was observed for most eukaryotic and some prokaryotic unicellular organisms.

The small range of α-particles necessitated the use of a mono-layer of yeast cells for irradiation: 0.02 ml of the cell suspension was placed on the surface of a non-nutrient agar, and the water from this drop of suspension was evaporated. The viability of the yeast cells after γ-irradiation was identical for cells on the agar surface and for the cells in the water suspension.

All irradiations were carried out in air at room temperature (20±2℃). Immediately after irradiation, part of the sample was plated on nutrient agar plates for the assay of colony-forming ability. Another part of the irradiated cell suspension was placed in conditions suitable for the LHR. After three days (delayed plating) their colony-forming ability was checked again. LHR was carried out in water suspension at 30℃. After the full LHR of cells irradiated with γ-rays at 1200 Gy and α-particles at 400 Gy, the suspension was again irradiated with the same increasing doses. This procedure was then repeated a third time. At the end of the treatment, the samples were further diluted and plated on nutrient agar to assess colony-forming ability.

The survival response was determined by colony counts at the end of 5.7 days of incubation at 30.C. Each data point represents the average survival on three to six Petri dishes, each containing 50~200 clones. Experimental points in all the figures have errors of 2% or less, that is, approximately the size of the points. Dose effect curves have been drawn by visually fitting the experimental points. Dosimetry, irradiation and

other details have been published previously [6-3, 6-23, 6-24]. To observe the recovery kinetics, another part of the irradiated cell suspensions and the untreated controls were placed under conditions suitable for the LHR, and their colony-forming ability was determined as a function of the incubation time in recovery conditions (delayed plating). LHR was carried out in a water suspension at 30℃ without constant agitation (the cell concentration was 106 cells/ml). The dose response curves and recovery kinetics were independent of whether the cell suspension was prepared with 0.07 M phosphate buffer or with distilled water. Survival response on immediate and delayed plating was determined on the basis of the colony counts obtained at the end of 5.7 days of incubation at 30℃. The counts were checked again after a further period to ensure that the final score had been reached. During the LHR process a number of the primary radiation damages are eliminated, resulting in an increased cell survival. This can be considered as a reduction of the initial dose D1 to a certain effective dose Deff(t) which is proportional to the mean number of the residual damages, both reparable and irreversible, after a recovery for t h. It has been demonstrated for yeast cells [6-19, 6-20] that the decrease in the effective dose Deff(t) with the recovery time t maybe described as follow

$$Deff\ (t) = D1\ [K + (1-K) \times e^{-\beta xt}, \qquad (1)$$

where β is the recovery constant that characterizes the probability of the recovery per unit time. In other words, the recovery constant is approximately equal to the fraction of the reversible radiation damage recovering per unit time. The fraction of radiation damage K is the irreversible component of radiation damage, which can be determined as

$$K = Deff(\infty) / D1, \qquad (2)$$

where Deff(∞) is the effective dose corresponding to the plateau of the recovery curve, which is proportional to the mean number of the irreversible damage. The ratio

$$K(t) = Deff(t) / D1. \quad (3)$$

reflects the relative part of the primary radiation damage that has not been repaired during t h of recovery. It follows from Eq. (1) that

$$\beta = (1/t) \ln[(Deff(t)-Deff(\infty)) / (D1-Deff(\infty))], \quad (4)$$

Designating

$$A(t) = (Deff(t)-Deff(\infty)) / (D1-Deff(\infty)), \quad (5)$$

we have

$$\beta = -\ln A(t) / t. \quad (6)$$

In biological terms, A(t) reflects the proportion of the reparable damage that has not been repaired after t h of recovery. Thus, knowing the survival and recovery curves after cell exposure to low- and high-LET radiation, one can calculate the corresponding values of Deff(t), Deff(∞), K(t), K, A(t), and b. In this paper the described mathematical approach will be used to quantify parameters of yeast-cell recovery from potentially lethal damage induced after repeated exposures to low- and high-LET radiations.

3. Results

Fig. 6-1 shows dose effect survival curves obtained immediately after γ-irradiation (closed circles) and after complete post-irradiation LHR (open circles) (A-C, left panel) as well as cell survival dependent on the duration of post-irradiation recovery (A-C, right panel). The results were obtained after the first (A), the second (B) and the third

(C) irradiation.

Similar data after expo-sure to α-particles are presented in Fig. 6-2. After each γ-exposure (1200 Gy) and full recovery, the percentage of surviving cells was reduced by about an order of magnitude. It is evident that the rate of cell recovery (A, C, right panel) gradually slowed down for 48 h, and that the survival curve, dependent of the recovery time, reached a plateau. These data are summarized in Table 6-1, which includes the following parameters of these curves: the mean lethal doses of γ- and α-irradiation after immediate and delayed plating, and the irreversible component K (Eq. (2)) of the radiation damage, as well as the recovery constant b after sparsely and densely ionizing radiation estimated by means of Eq. (4), respectively. The results of our calculations are presented in Table 1 after the first, second, and third exposure to both types of radiation. In this table the calculated values of the mean lethal dose are also included. The mean lethal dose is the dose required to reduce cell survival to e = 2.72 on a straight part of the survival curve, depicted on a semi-log scale. This value was used for the RBE calculation. The shape of the survival curves was sigmoid after the first irradiation, both with γ-rays and α-particles. After the subsequent irradiations the survival curves became exponential and the mean lethal doses, characterizing the slope of the survival curves, only slightly depend on the number of subsequent irradiations. These data allowed us to calculate RBE values as the ratio of D0(γ)/D0(α); they were 2.9, 2.4, and 2.6 after the first, second and third irradiations. This means that within possible experimental errors the RBE of α-particles does not depend on the repeated exposures. For low-LET radiation the extent of recovery decreased after re-exposures, consequently the irreversible component of radiation damage increased from 0.45 after the first, to 0.66 after the third exposure. This effect was much more pronounced after exposure to α-particles when irreversible component increased from 0.47 after the first exposure to 1.00 after the third one. The value K = 1.0 means that all potentially lethal damage is completely irreversible. How-ever, it does not indicate that there are no survivors after the third exposure with higher density radiation. Undamaged cells without potentially lethal and lethal damage are survivors. It means that after the third exposure to α-particles only irreversible damage was produced.

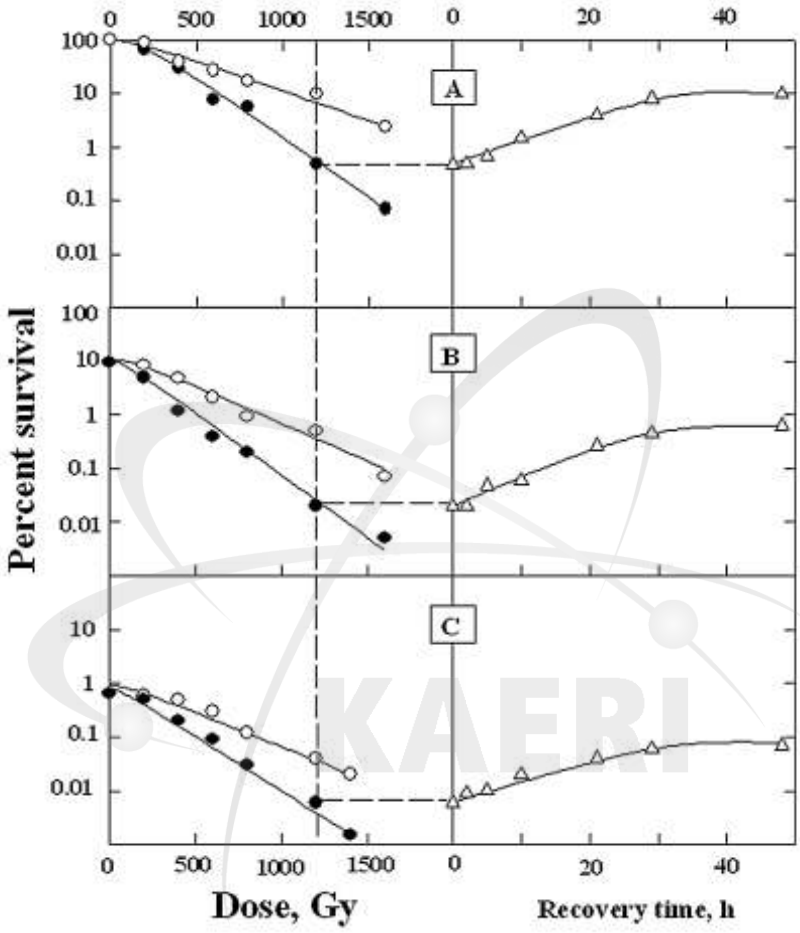

Fig. 6-1. Survival curves ((A)-(C), left panel) obtained immediately after γ-irradiation (closed circles) and after complete post-irradiation recovery (open circles); cell survival((A)-(C), right panel); (A).the first irradiation; (B).the second exposure; (C).the third exposure. Experiments were performed with diploid *S. cerevisiae* yeast cells, strainXS800.

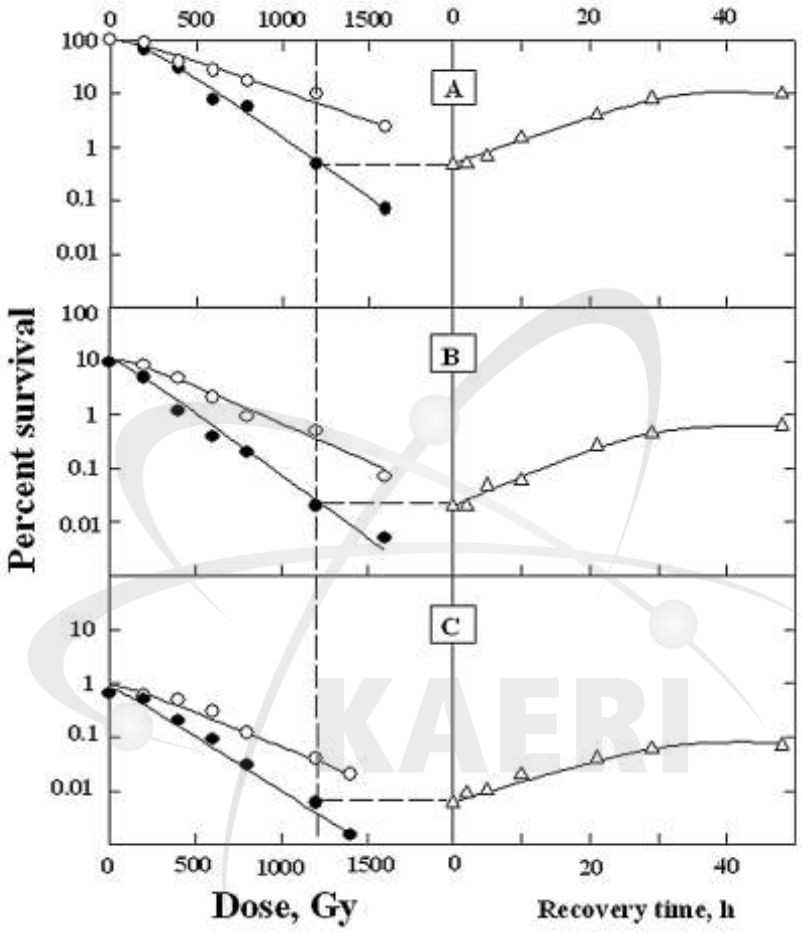

Fig. 6-2. As in Fig. 6-1, but after exposure to α-particles.

Table 6-1. The parameters characterizing the process of radiation recovery

Type of radiation	number of exposure	D0 (Gy) before LHR	D0 (Gy) after LHR	K	β ($1h^{-1}$)
ɣ-rays	1	189	387	0.45	0.055
	2	172	366	0.46	0.055
	3	215	301	0.58	0.055
α-particles	1	65	107	0.47	0.041
	2	70	107	0.77	0.041
	3	81	81	1.00	0.041

The data presented in Table 6-1 shows that the probability of recovery does not depend on the number of repeated exposures and that it somewhat decreases after exposures to high-LET radiation. The irreversible component of the radiation damage increases after the third irradiation with low-LET radiation, and significantly increases after exposure to high-LET radiation. Moreover, in the latter case the recovery after the third exposure was completely stopped. From these results, the slowing down of the process of recovery and the reduction in the extent to which the cells recover after repeated exposures can be easily seen. This effect was particularly pronounced after exposure to high-LET radiation. Actually, after re-exposure the process of liquid-holding recovery slowed down dramatically, and completely stopped after the third exposure.

4. Discussion

It was shown previously [6-3, 6-13] that RBE of densely ionizing radiation correlates with the ability of cells to recover from the damage inflicted by the radiation. This concept was based on numerous data showing that RBE of high-LET radiation is significantly higher for cells capable of recovery, compared with the values of RBE revealed for radiosensitive mutants that are defective in the repair process. These data are available for cells of different origin [6-3~6-6]. It has been shown that the mechanism of increased RBE values was due to the decrease in the ability of the cells to recover from the damage caused by high-LET radiation [6-7~6-10]. The well-known radiobiological data [6-11, 6-12] suggest that recovery may be inhibited due to the impairment of the recovery process itself, i.e. due to decrease in the recovery constant, which describes the probability of recovery per unit time. Another reason for the reduced ability of the cells to recover from the radiation damage may be an increase in the proportion of irreversible damage. A detailed analysis of this problem [6-23] showed that the recovery process itself is not impaired after densely ionizing radiation, and that the enhanced RBE of the high-LET radiation may be caused by the

increased yield of irreversible damage. A parent diploid strain and its radiosensitive mutants showed the same probability for recovery from radiation damage. Thus, the mechanism of the enhanced radiosensitivity of the mutant cells defective in some repair systems may not be related to the damage in cell recovery, but with the production of some kind of radiation damage from which cells are incapable to recover. In connection with these results, the ability of cells to recover from repeated exposures to low- and high-LET radiation was studied in this paper. Diploid yeast cells were irradiated with γ-rays and α-particles. Survival curves immediately after radiation and the kinetics of the LHR were measured. When the irradiated cells were completely recovered, they were subjected to irradiation and post irradiation recovery again. The procedure was repeated three times. It should be noted that after repeated exposures the survival curve form have changed from the initial sigmoidal form to the exponential one, although the slope of the survival curves have changed insignificantly after the α- and γ-irradiations. In this regard, RBE of α-particles did not depend in a great extent on the number of repeated irradiations (2.9, 2.4, 2.6 after the first, second and third exposure). The new results obtained in this study, indicate that the repeated exposures to high-LET radiation result in a big decrease in the ability of cells to recover from potentially lethal damage due to the formation of irreversible damage from which the cells are not able to recover. The increase in the proportion of primary radiation damage after repeated exposures may occur for two reasons; either the formation of damage that could not be repaired at all, or due to impairment of the recovery process itself. Both these possibilities have been considered in this study. It is evident from the data presented that the irreversible component of radiation damage increased after repeated exposures with gamma-rays from 0.4 after the first irradiation to 0.7 after the third exposure. This effect was more noticeable after densely ionizing radiation exposure, the corresponding values being 0.5 and 1.0. The second possibility was also analyzed. Our results indicated that regardless of the number of repeated irradiations, the recovery constant b varies insignificantly for both types of radiation. The discontinuity of cell recovery after reaching a plateau of the recovery curve is unlikely due to the exhaustion of the relevant metabolites or recovery enzymes because the

LHR process continued after the first, second and third exposure to low-LET radiation. In the case of α-particles the slowing-down and complete stopping of the LHR was more pronounced even after the second exposure. This means that the process of recovery is not impaired itself after repeated irradiations with low- and high-LET radiation. Actually, the recovery constant was shown to be slightly dependent on radiation quality: it changed from 0.055 h^{-1} for γ-rays to 0.041 h^{-1} for α-particles. In other words, 5.5 and 4.1% of the damage available for repair were recovered every hour after γ- and α-irradiation. It is worth noting that in the detailed study of liquid-holding recovery kinetics in wild-type and radiosensitive mutants of the yeast *Saccharomyces* exposed to low- and high-LET radiations, the probability of recovery was identical after γ- and α-irradiation for eight yeast strains and varied within the range 0.05~1.00 h^{-1} [6-23]. The results obtained in this study are close to that range. It may suggest that the process of recovery from potentially lethal radiation damage itself is not damaged after repeated irradiations both with low- and high-LET radiations, and that the decrease in the ability of the cell to recover from the radiation damage is completely explained by the increased proportion of irreversibly damaged cells. In conclusion, it is of interest to note that in many investigations carried out in the biophysical laboratory it was shown that synergistic interaction of various environmental factors was related with production of additional effective damage due to interaction of some sub-lesions rat her than the impairmen to fcell-recovery capacity itself [6-13, 6-19~6-21]. The identical slopes of the survival curves obtained in this study after repeated exposures to γ-rays and α-particles suggest that these sub-lesions are either eliminated or repaired during the LHR.

5. Conclusions

From the results of this study, conclusions could be drawn out as follows. Repeated exposures to high-LET radiation result in a dramatic decrease in cell capability to recover from potentially lethal damage, due to formation of irreversible damage from

which cells are not able to recover. This effect was expressed to a greater extent upon exposure to α-particles. After repeated exposures of diploid yeast cells to low- and high-LET ionizing radiation, the recovery constant characterizing the probability of cell recovery per unit time is independent of the number of repeated exposures. Finally, the RBE of α-particles was insignificantly dependent on the number of repeated exposures.

KAERI

제 3 장 결론 및 건의사항

KAERI

제 3 장 결 론

“방사선의 생물분자 구조변환 및 복합작용 연구” 과제의 수행을 통하여 국가 방사선 핵심연구에 필요한 기반기술을 확하고 기존의 기술을 개선·발전시키고자 하였으며 다음과 같은 주요 내용과 범위가 연구개발에 포함되었다.

○ 방사선유발 염색체 이상 (dicentrics)을 이용한 생물선량 평가
○ 분자지표 (γ-H2AX)를 이용한 분자선량평가 기반연구
○ 방사선조사에 따른 세포신호전달 및 세포사멸 과정 분석연구
○ 방사선 노출에 따른 세포생존율 측정 검증
○ 퀘세틴 및 배당체의 방사선 방호 검증 및 연구
○ 세포에 대한 고 LET 및 저 LET 방사선의 복합작용

이러한 연구개발의 내용과 범위는 국내외 연구 환경에 대한 조사·분석을 통하여 이뤄진 것이다. 국제원자력기구, 국제방사선방호위원회 등은 새로운 방사선 생물방호를 위한 새로운 개념과 변화된 가이드라인을 제시하고 있기 때문에 이에 부합하는 연구방향을 따른 것이다. 특히, 방사선 단일 조건에 의한 생물반응에 관한 연구에서 벗어나서 방사선과 다른 물리·화학적 요인이 복합적으로 생물체에 미치는 영향을 연구하고 해석하는 기술은 국제적 우위기술로 이를 더욱 발전시키기 위한 노력이 이워졌다. 방사선 융·복합 기술은 단순하게 방사선을 조사하고 그 결과를 이용하던 단편적 기술의 한계를 극복하고 새로운 기술로 도약할 수 있는 다제간 신기술로서 다양한 이용범위를 가지며 산업적 파급효과가 높은 동시에 경제적 효과가 큰 강점 기술이다. 이온화 방사선의 에너지에 따라 방사선에 노출된 생물 개체 및 생체 물질 분자에서 나타나는 반응은 다양하다. 이를 연구한 결과는 저명학술지에 논문으로 게재하여 연구 성과의 우수성과 연구수행의 성실성을 입증하였다. 연구결과는 후속 연구를 통해 더욱 개선되고 발전될 것이며 향후 새로운 연구과제 도출 및 수행을 위한 동기부여는 물론 기반기술로 제공될 것으로 전망된다.

이온화 방사선의 복합 생물반응 평가기술은 환경, 의·약학, 생명과학, 산업 분야 등 폭넓은 분야에 적용 가능한 핵심기술로 평가되고 있으며 방사선의 긍정적 이용효율 증

대를 위한 필수 요소기술이다. 연구결과를 개선하여 방사선 이용기술의 고도화를 위한 연구개발 및 응용 분야의 기반을 확립하고 방사선 복합 생물영향 해석 신기술 자립 및 방사선민감도 해석 자료 구축을 통한 과학기술 발전기여와 함께 국제 기술우위를 확보할 수 있을 것이다. 장기적으로는 방사선작업종사자 및 노출자 (사고 피폭자 및 희생자 포함)에 대한 생물반응의 retrospective dosimetry 기술을 제공과 함께 방사선 생물방호 원천기술의 수립과 함께 방사선에 대한 생물반응 해석과 응응 기술의 진일보에 기여할 것으로 기대된다.

제4장 참고문헌

KAERI

제 4 장 참고문헌

[제 1 절]

1-1. Amundson SA, Bittner M, Meltzer P, Trent J, Fornace AJ Jr. (2001). Biological indicators for the identification of ionizing radiation exposure in humans. Exper Rev Mol Diagn. 1(2): 89-97.

1-2. Ainsbury EA, Barquinero JF. (2009). Biodosimetric tools for a fast triage of people accidentally exposed to ionizing radiation, Statistical and computational aspects. Ann Ist Super Sanita. 45: 307-312.

1-3. Senthamizhchelvan S, Pant GS, Rath GK, Julka PK, Nair O, Joshi RC, Malhotra A, Pandey RM. (2007). Biodosimetry using chromosome aberrations in human lymphocytes. Rad Prot Dosim. 123(2): 241-245.

1-4. Lamadrid Boada AI, Romero Aguilera I, Terzoudi GI, Gonzalez Mexa JE, Pantelias G, Garcia O. (2013). Rapid assessment of high-dose radiation exposures through scoring of cell-fusion-induced premature chromosome condensation and ring chromosomes. Mutat Res. 757: 45-51.

1-5. Stimpson KM, Matheny JE, Sullivan BA. (2012). Dicentric chromosomes: unique models to study centromere function and inactivation. Chromos Res. 20: 595-605.

1-6. Bender MA, Gooch PC, Types and rates of X-ray-induced chromosome aberrations in human blood irradiated *in vitro.* (1962). Proc Natl Acad Sci (USA). 48: 522-532.

1-7. Schroder H, Heimers A. (2002). Chromosome aberrations induced in human lymphocytes by *in vitro* and *in vivo* X-rays. Mutat Res. 517: 167-172.

1-8. International Atomic Energy Agency. (2011). Cytogenetic dosimetry: applications in preparedness for and response to radiation emergencies. Vienna, IAEA.

1-9. Papworth DG, Savage JRK. (1975). Curve fitting by maximum likelihood, radiation-induced chromosomal aberrations in tradescantia: dose response curves. Radiat Bot. 15: 87-140.

1-10. Romm H, Oestreicher U, Kulka U. (2009). Cytogenetic damage analysed by the dicentric assay. Ann Ist Super Sanita. 45: 251-259.

1-11. Sevan 'kaev AV, Kozlov VM, Guseev GG, Izmailova NN (Ed.). (1974). Frequency of spontaneous chromosome aberrations in the culture of human lymphocytes. Genetics (USSR). 10: 114-120.

1-12. Ganguly BB. (1993). Cell division, chromosomal damage and micronucleus formation in peripheral lymphocytes of healthy donors related to donor's age. Mutat Res. 295: 135-48.

1-13. Al-Hadyan K, Elewisy S, Moftah B, Shoukri M, Alzahrany A, Alsbeih G. (2014). Establishing cytogenetic biodosimetry laboratory in Saudi Arabia and producing preliminary calibration curve of dicentric chromosomes as biomarker for medical dose estimation in response to radiation emergencies. Biotech. DOI 10.1007/s13205-014-0217-x.

1-14. Ryu TH, Roh C, Kim JK. Cytokinesis-block micronucleus (CBMN) assay in human lymphocytes irradiated in vitro with gamma-rays. The Joint International Symposium on EPR Dosimetry and Dating and the International Conference on Biological Dosimetry. Mar, 24-28, 2013. Leiden, Netherlands.

[제 2 절]

2-1. Rogakou EP, Pilch DR, Orr AH, Ivanova VS, Bonner WM (1998) DNA double-stranded breaks induce histone H2AX phosphorylation on serine 139. J Biol Chem, 273: 5858-5868.

2-2. Dickey JS, Redon CE, Nakamura AJ, Baird BJ, Sedelnikova OA, Bonner WM (2009) H2AX: functional roles and potential applications. Chromosoma, 118: 683-692.

2-3. Löbrich M, Shibata A, Beucher A, Fisher A, Ensminger M, Goodarzi AA, Barton O, Jeggo PA (2010) γ-H2AX foci analysis for monitoring DNA double-strand break repair. Cell Cycle, 9: 662-669.

2-4. Kuo LJ and Yang LX (2008) γ-H2AX - a novel biomarker for DNA double-strand breaks. In Vivo, 22: 305-310.

2-5. Horn S, Barnard S, Rothkamm K (2011) Gamma-H2AX-Based Dose Estimation for Whole and Partial Body Radiation Exposure. PLoS One, 9: e25113.

2-6. Sak A, Grehl S, Erichsen P, Engelhard M, Granna A, Levegrun S, Pottgen C, Groneberg M, Stuschke M (2007) γ-H2AX foci formation in peripheral blood lymphocytes of tumor patients after local radiotherapy to different sites of the body: Dependence on the dose-distribution, irradiated site and time from start of treatment. Int J Radiat Biol, 83: 639-652.

2-7. Pope IA, Barber PR, Horn S, Ainsbury E, Rothkammb K, Vojnovic B (2011) A portable microfluidic fluorescence spectrometer device for γ-H2AX-based biological dosimetry. Radiat Measurements, 46: 907-911.

2-8. Jakoba B and Durante M (2012) Radiation Dose Detection by Imaging Response in Biological Targets. Radia Res, 177: 524-532.

2-9. Rogakou EP, Pilch DR, Orr AH, Ivanova VS, Bonner WM (1998) DNA double-stranded breaks induce histone H2AX phosphorylation on serine 139. J Biol Chem, 273: 5858-5868.

2-10. Avondoglio D, Scott T, Kil WJ, Sproull M, Tofilon PJ, Camphausen K (2009) High throughput evaluation of gamma-H2AX. Radiat Oncol, 4: 1-5.

2-11. Redon CE, Nakamura AJ, Martin OA, Parekh PR, Weyemi US, Bonner WM (2011) Recent developments in the use of ɣ-H2AX as a quantitative DNA double-strand break biomarker. Aging, 3: 168-174.

2-12. Rogakou EP, Boon C, Redon C, Bonner WM (1999) Megabase Chromatin Domains Involved in DNA Double-Strand Breaks. J Cell Biol, 146: 905-915.

2-13. Nakamura A, Sedelnikova OA, Redon C, Pilch DR, Sinogeeva NI, Shroff R, Lichten M, Bonner WM (2006) Techniques for gamma-H2AX detection. Methods Enzymol, 409: 236-250.

2-14. Johansson P, Muslimovic A, Hultborn R, Fernström E, Hammarsten O (2011) In-solution staining and arraying method for the immunofluorescence detection of ɣ-H2AX foci optimized for clinical applications. BioTechniques, 51: 185-189.

[제 3 절]

3-1. Giaccia AJ, Kastan MB. The complexity of p53 modulation: emerging patterns from divergent signals. Genes Dev. 1998 (19):2973-2983.

3-2. Mirzayans R, Andrais B, Scott A, Wang YW, Murray D. Ionizing radiation-induced responses in human cells with differing TP53 status. Int J Mol Sci. 2013 (11):22409-22435.

3-3. Fei P, El-Deiry WS. P53 and radiation responses. Oncogene. 2003 (37):5774-5783.

3-4. Shao Y, Gao Z, Marks PA, Jiang X. Apoptotic and autophagic cell death induced by histone deacetylase inhibitors. Proc Natl Acad Sci. 2004 (52):18030-18035.

3-5. Yang XH, Sladek TL, Liu X, Butler BR, Froelich CJ, Thor AD. Reconstitution of caspase 3 sensitizes MCF-7 breast cancer cells to doxorubicin- and etoposide-induced apoptosis. Cancer Res. 2001 (61):348-354.

3-6. Kagawa S, Gu J, Honda T, McDonnell TJ, Swisher SG, Roth JA, Fang B. Deficiency of caspase-3 in MCF7 cells blocks Bax-mediated nuclear fragmentation but not cell death. Clin Cancer Res. 2001 (5):1474-1480.

3-7. Sasaki M, Miyakoshi M, Sato Y, Nakanuma Y. Autophagy mediates the process of cellular senescence characterizing bile duct damages in primary biliary cirrhosis. Lab Invest. 2010 (6):835-843.

3-8. Mizushima N, Levine B, Cuervo AM, Klionsky DJ. Autophagy fights disease through cellular self-digestion. Nature. 2008 (718):1069-1075.

3-9. Ouyang L, Shi Z, Zhao S, Wang FT, Zhou TT, Liu B, Bao JK. Programmed cell death pathways in cancer: a review of apoptosis, autophagy and programmed necrosis. Cell Prolif. 2012 (6):487-498.

3-10. Li T, Kon N, Jiang L, Tan M, Ludwig T, Zhao Y, Baer R, Gu W. Tumor suppression in the absence of p53-mediated cell-cycle arrest, apoptosis, and senescence. Cell. 2012 (6):1269-1283.

3-11. Amundson SA, Myers TG, Fornace AJ Jr. Roles for p53 in growth arrest and apoptosis: putting on the brakes after genotoxic stress. Oncogene. 1998 (17):3287-3299.

3-12. Agarwal ML, Agarwal A, Taylor WR, Stark GR. P53 controls both the G2/M and G1 cell cycle checkpoints and mediates reversible growth arrest in human fibroblasts. Proc Natl Acad Sci. 1995 (92):8493-8497.

3-13. Vousden KH, Lane DP. p53 in health and disease. Nat Rev Mol Cell Biol. 2007 (4):275-283.

3-14. Sablina AA, Budanov AV, Ilyinskaya GV, Agapova LS, Karvchenko JE, Chumakov PM. The antioxidant function of the p53 tumor suppressor. Nat Med. 2005 (11):1306-1313.

3-15. Polyak K, Xia Y, Zweier JL, Kinzler KW, Vogelstein B. A model for p53-induced apoptosis. Nature. 1997 (389):300-305.

3-16. Macip S, Igarashi M, Berggren P, Yu J, Lee SW, Aaronson SA. Influence of induced Reactive Oxygen Species in p53-mediated cell fate decisions. Mol Cell Biol. 2003 (23):8576-8585.

3-17. Roninson IB. Tumor cell senescence in cancer treatment. Cancer Res. 2003 (11):2705-2715.

3-18. Zhang XP, Liu F, Cheng Z, Wang W. Cell fate decision mediated by p53 pulses. Proc Natl Acad Sci. 2009 (30):12245-12250.

3-19. Zhang XP, Liu F, Wang W. Two-phase dynamics of p53 in the DNA damage response. Proc Natl Acad Sci. 2011 (22):8990-8995.

3-20. Elmore S. Apoptosis: a review of programmed cell death. Toxicol Pathol. 2007 (4):495-516.

3-21. Mirzayans R, Scott A, Cameron M, Murray D. Induction of accelerated senescence by gamma radiation in human solid tumor-derived cell lines expressing wild-type TP53. Radiat Res. 2005 (1):53-62.

3-22. Li DD, Sun T, Wu XQ, Chen SP, Deng R, Jiang S, Feng GK, Pan JX, Zhang XS, Zeng YX, Zhu XF. The inhibition of autophagy sensitises colon cancer cells with wild-type p53 but not mutant p53 to topotecan treatment. PLoS One. 2012 (9):e45058.

3-23. Liang B, Kong D, Liu Y, Liang N, He M, Ma S, Liu X. Autophagy inhibition plays the synergetic killing roles with radiation in the multi-drug resistant

SKVCR ovarian cancer cells. Radiat Oncol. 2012 (7):213.

3-24. Paglin S, Hollister T, Delohery T, Hackett N, McMahill M, Sphicas E, Domingo D, Yahalom J. A novel response of cancer cells to radiation involves autophagy and formation of acidic vesicles. Cancer Res. 2001 (2):439-444.

3-25. Cheng G, Kong D, Hou X, Liang B, He M, Liang N, Ma S, Liu X. The tumor suppressor, p53, contributes to radiosensitivity of lung cancer cells by regulating autophagy and apoptosis. Cancer Biother Radiopharm. 2013 (2):153-159.

3-26. Wilson EN, Bristol ML, Di X, Maltese WA, Koterba K, Beckman MJ, Gewirtz DA. A switch between cytoprotective and cytotoxic autophagy in the radiosensitization of breast tumor cells by chloroquine and vitamin D. Horm Cancer. 2011 (5):272-285.

[제 4 절]

4-1. Lewanski CR and Gullick WJ (2001) Radiotherapy and Cellular signaling. *Lancet Oncol*, ***2:366-370.***

4-2. Debenham BJ, Hu KS, Harrison LB (2013) Present status and future directions of intraoperative radiotheraphy. Lancet Oncol, 13:e457-464.

4-3. Schmidt N, Büttner N, Thimme R (2013) Perspectives on immunotherapy for hepatocellular carcinoma. Dtsch Med Wochenschr, 138:740-744.

4-4. Xia J, Gao J, Inagaki Y, Kokudo N, Nakata M, Tang W (2013) Flavonoids as potential anti-hepatocellular carcinoma agents: Recent approaches using HepG2 cell line. Drug Discov Ther, 7:1-8.

4-5. Mirzayans R, Andrais B, Scott A, Wang YM, Murray D (2013) Ionizing radiation-induced responses in human cells with differing TP53 status. Int J Mol Sci, 13:22409-22435.

4-6. Eriksson D, Stigbrand T (2010) Radiatio-induced cell death mechanisms. Tumour Biol, 31:363-372.

4-7. Banáth JP, Macphal SH, Olive PL (2004) Radiation sensitivity, H2AX phosphorylation, and kinetics of repair of DNA strand breaks in irradiated cervical cancer cell lines. Cancer Res, 64:7144-7149.

4-8. Mahrhofer H, Bürger S, Oppitz U, Flentje M, Djuzenova CS (2006) Radiation induced DNA damage and damage repair in human tumor and fibroblast cell lines assessed by histone H2AX phosphorylation. Int J Radiat Oncol Biol Phys, 64:573-580.

4-9. Mariotti LG, Pirovano G, Savage KI, Ghita M, Ottolenghi A, Prise KM, Schettino G (2013) Use of the ɣ-H2AX assay to investigate DNA repair dynamics following multiple radiation exposures. PLoS One 8:e79541.

4-10. Raffoul JJ, Wang Y, Kucuk O, Forman JD, Sarkar FH, Hillman GG (2006) Genistein inhibits radiation-induced activation of NF-kappaB in prostate cancer cells promoting apoptosis and G2/M cell cycle arrest. BMC Cancer 6:107.

4-11. Held KD (1997) Radiation-induced apoptosis and its relationship to loss of clonogenic survival. Apoptosis 2:265-82.

4-12. Karhikeyan S, Kanimozhi G, Prasad NR, Mahalakshmi R (2011) Radiosensitizing effect of ferulic acid on human cervical carcinoma cells in vitro. Toxicol In Vitro 25:1366-1375.

4-13. Guo J, Zhang Y, Zeng L, Liu J, Liang J, Guo G (2013) Salvianic acid A protects L-02 cells against γ-irradiation-induced apoptosis via the scavenging of reactive oxygen species. Environ Toxicol Pharmacol 35:117-130.

4-14. Zoberi I, Bradbury CM, Curry HA, Bisht KS, Goswami PC, Roti Roti JL, Gius D (2002) Radiosensitizing and anti-proliferative effects of resveratrol in two human cervical tumor cell lines. Cancer Lett 175:165-173.

4-15. Lin C, Yu Y, Zhao HG, Yang A, Yan H, Cui Y (2012) Combination of quercetin with radiotherapy enhances tumor radiosensitivity in vitro and in vivo. Radiother Oncol 104:395-400.

4-16. Kulak U, Schaffer M, Siefert A, Schaffer PM, Olsner A, Kasseb K, Hofstetter A, Dühmke E, Jori G (2003) Photofrin as a radiosensitizer in an in vitro cell survival assay. Biochem Biophys Res Commun. 311:98-103.

4-17. Jauregui HO, Hayner NT, Driscoll JL, Williams- Holland R, Lipsky MH, Galletti PM (1981) Trypan blue dye uptake and lactate dehydrogenase in adult rat hepatocytes freshly isolated cells, cell suspensions, and primary monolayer cultures. In vitro 17:1100-1110.

4-18. Mosmann T (1983) Rapid colorimetric assay for cellular growth and survival: application to proliferation and cytotoxicity assays. J Immunol Methods 65:55-63.

4-19. Franken NA, Rodermond HM, Stap J, Haveman J, van Bree C (2006) Clonogenic assay of cells in vitro. Nat Protoc 1:2315-2319.

4-20. Verheij M, Bartelink H (2000) Radiation-induced apoptosis. Cell Tissue Res 301:133-42.

4-21. Roem NW, Rodgers GH, Hatfield SM, Glasebrook AL (1991) An improved colorimetric assay for cell proliferation and viability utilizing the tetrazolium salt XTT. J Immunol Methods 142:257-265.

4-22. Chen X, Zhong Z, Xu Z, Chen L, Wang Y (2011) No protective effect of curcumin on hydrogen peroxide-induced cytotoxicity in HepG2 cells. Pharmacol Rep 63:724-732.

4-23. Szuster-Ciesielska A, Kandefer-Szerszeń M (2005) Protective effects of botulin and betulinic acid against ethanol-induced cytotoxicity in HepG2 cells. Pharmcol Rep 57:588-595.

4-24. Jiao HL, Ye P, Zhao BL (2003) Protective effects of green tea polyphenols on human HepG2 cells against oxidative damage of fenofibrate. Free Radic Biol Med 35:1121-1128.

4-25. Sohn JH, Han KL, Lee SH, Hwang JK (2005) Protective effects of panduratin A against oxidative damage of tert-butylhydroperoxide in human HepG2 cells. Biol Pharm Bull 28:1083-1086.

[제 5 절]

5-1. A.G. Chmielewski, M. Haji-Saeid, Radiation technologies: past, present and future, Radiat.Rhys. Chem. 71 (2004) 16-20.

5-2. J.L. Ryan, Ionizing radiation: The good, the bad and the ugly, J. Invest. Dermatol. 132 (2012) 985-993.

5-3. J.E. Moulder, Post irradiation approaches to treatment of radiation injuries in the context of radiological terrorism and radiation accidents: a review, Int. J. Radiat. Biol. 80 (2004) 3-10.

5-4. K.D. Held, Radiation-induced apoptosis and its relationship to loss of clonogenic survival, Apoptosis, 2 (1997) 265-282.

5-5. P.A. Riley, Free radicals in biology: oxidative stress and effects of ionizing radiation, Int. J. Radiat. Biol. 65 (1994) 27-33.

5-6. S.J. Hosseinimehr, Trends in the development of radioprotectic agents, Drug Discov. Today. 12 (2007) 794-805.

5-7. R.J. Ormsby, M.D. Lawrence, B.J. Blyth, K. Bexis, E. Bezak, J.S. Murley, D.J. Grdina, P.J. Sykes, Protection from radiation-induced apoptosis by the radioprotector amifostine (WR-2721) is radiation dose dependent, Cell Biol. Toxicol. 30 (2014) 55-66.

5-8. V.S. Kuntić, M.B. Stanković, Z.B. Vujić, J.S. Brborić, S.M. Uskoković-Marković, Radioprotectors-the evergreen topic, Chem. Biodivers. 10 (2013) 1791-1803.

5-9. J.F. Weiss, M.R. Landauer, Protection against ionizing radiation by antioxidant nutrients and phytochemicals, Toxicology. 189 (2003) 1-20.

5-10. C.C. Araujo, L.L. Leon, Biological activities of Curcuma longa L., Mem. Inst. Oswaldo. Cruz. 96 (2001) 723-728.

5-11. R.K. Maheshwari, A.K. Singh, J. Gaddipati, R.C. Srimal, Multiple biological activities of curcumin: A short review, Life Science. 78 (2006) 2081-2087.

5-12. B.B. Aggarwal, A. Kumar, A.C. Bharti, Anticancer potential of curcumin: preclinical and clinical studies, Anticancer Res. 23 (2003) 363-398.

5-13. B. Joe, M. Vijaykumar, B. Lokesh, Biological properties of curcumin-cellular and

molecular mechanisms of action, Crit. Rev. Food Sci. Nutr. 44 (2004) 97-111.

5-14. S. Prasad, A.K. Tyagi, B.B. Aggarwal, Recent developments in delivery, bioavailability, absorption and metabolism of curcumin: the golden pigment from golden spice, Cancer Res.Treat. 46(2014) 2-18.

5-15. S.K. Abraham, L. Sarma, P.C. Kesavan, Protective effects of chlorogenic acid, curcumin and β-carotene against ɣ-radiation-induced in vivo chromosomal damage, Mutat. Res. 303 (1993) 109-112.

5-16. M. Srinivasan, N. Rajendra Prasad, V.P. Menon, Protective effect of curcumin on ɣ-radiation induced DNA damage and lipid peroxidation in cultured human lymphocytes, Mutat. Res. 611 (2006) 96-103.

5-17. S. Knasmuller, V. Mersch-Sundermann, S. Kevekordes, F. Darroudi, W.W. Huber, C. Hoelzl, J. Bichler, B.J. Majer, Use of human-derived liver cell lines for the detection of environmental and dietary genotoxicants; current state of knowledge, Toxicology. 198(2004) 315-328.

5-18. V. Mersch-Sundermann, S. Knasmuller, X.J. Wu, F. Darroudi, F. Kassie, Use of a humanderived liver cell line for the detection of cytoprotective, antigenotoxic and cogenotoxic agents, Toxicology. 198 (2004) 329-340.

5-19. N. Sebastià, M. Almonacid, J.I. Villaescusa, J. Cervera, E. Such, M.A. Silla, J.M. Soriano, A. Montoro, Radioprotective activity and cytogenetic effect of resveratrol in human lymphocytes: an in vitro evaluation, 51 (2013) 391-395.

5-20. N.A. Franken, H.M. Rodermond, J. Stap, J. Haveman, C. van Bree, Clonogenic assay of cells in vitro, Nat. Protoc. 1 (2006) 2315-2319.

5-21. R.R. Tice, E. Agurell, D. Anderson, B. Burlinson, A. Hartmann, H. Kobayashi, Y. Miyamae, E. Rojas, J.C. Ryu, Y. F. Sasaki, Single cell gel/comet assay: guidelines for in vitro and in vivo genetic toxicology testing, Environ. Mol. Mutagen. 35 (2000) 206-221.

5-22. J. Cadet, M. Berger, T. Douki, R. Ravanat, Oxidative damage to DNA: formation, measurement and biological significance, Rev. Physiol. Biochem. Pharmacol. 31 (1997) 1-87.

5-23. R. Teoule, Radiation-induced DNA damage and its repair, J. Radiat. Biol. 51

(1987) 573-589.

5-24. A.R. Collins, V.L. Dobson, M. Dušinská, G. Kennedy, R. Stětina, The Comet assay: what can it really tell us?, Mutat. Res. 375 (1997) 183-193.

5-25. P.V. Olive, DNA damage and repair in individual cells: applications of the Comet assay in radiobiology, Int. J. Radiat. Biol. 75 (1999) 395-405.

5-26. M. Verheij, H. Bartelink, Radiation-induced apoptosis, Cell Tissue Res. 301 (2000) 133-142.

5-27. W.P. Roos, B. Kaina, DNA damage-induced cell death by apoptosis, Trends Mol. Med. 12 (2006) 440-450.

5-28. A. Duvoix, R. Blasius, S. Delhalle, M. Schnekenburger, F. Morceau, E. Hery, M. Dicato, M. Diederich, Chemopreventive and therapeutic effects of curcumin, 233 (2005) 181-190.

5-29. J.C. Lee, P.A. Kinniry, E. Arguiri, M. Serota, S. Kanterakis, S. Chatterjee, C.C. Solomides, P. Javvadi, C. Koumenis, K.A. Cengel, M. Christofidou-Solomidou, Radiat. Res. 173 (2010) 590-601.

[제 6 절]

6-1. R.H. Haynes, The interpretation of microbial inactivation and recovery phenomena, Radiat. Res. 6 (1966) 1- 29.

6-2. T. Alper, Cell death and its modification: the role of primary lesions in membranes and DNA, in: Biophysical Aspects of Radiation Quality, IAEA, Vienna, 1971, pp. 171- 184.

6-3. V.G. Petin, N.M. Kabakova, RBE of densely ionizing radiation for wild-type and radiosensitive mutants of yeast, Mutat. Res. 82 (1981) 285- 294.

6-4. M. Frankenberg-Schwager, D. Frankenberg, R. Harbich, Repair of DNA double-strand breaks as a determinant of RBE of alpha-particles, Br. J. Cancer 49 (VI)(1984) 169- 173.

6-5. J.D. Shadley, J.L. Whitlock, R.W. Atcher, J. Tang, J.L. Schwartz, The effect of radon daughter _-particle irradiation in K1 and xrs-5 CHO cell lines, Mutat. Res. 248(1991) 73- 83.

6-6. W.K. Weyrather, S. Ritte, M. Scholz, G. Kraft, RBE for carbon track-segment irradiation in cell lines of differing repair capacity, Int. J. Radiat. Biol. 75 (1999)1357- 1364.

6-7. M.A. Ritter, J.E. Cleaver, C.A. Tobias, High-LET radiations induce a large proportion of non-rejoining DNA breaks, Nature 266 (1977) 653- 655.

6-8. D. Blöcher, DNA double-strand break repair determines the RBE of _-particles, Int. J. Radiat. Biol. 54 (1988) 761- 771.

6-9. J. Heilmann, H. Rink, G. Taucher-Scholz, G. Kraft, DNA strand break induction and rejoining and cellular recovery in mammalian cells after heavy-ion irradiation, Radiat. Res. 135 (1993) 46- 55.

6-10. B. Stenerlöw, E. Höglund, J. Carlsson, E. Blomquist, Rejoining of DNA fragments produced by radiations of different linear energy transfer, Int. J. Radiat. Biol. 76(2000) 549- 557.

6-11. V.I. Korogodin, Problems of Postirradiation Recovery, Atomizdat, Moscow, 1966.

6-12. V.I. Korogodin, The study of post-irradiation recovery of yeast: the 'premolecular

period', Mutat. Res. 289 (1993) 17- 26.

6-13. V.G. Petin, Genetic Control of Cell Radiosensitivity Modification, Energoatomiz-dat, Moscow, 1987.

6-14. M. Frankenberg-Schwager, R. Harbich, S. Beckonert, D. Frankenberg, Half-life for DNA double-strand break rejoining in yeast can vary by more than an order of magnitude depending on the irradiation conditions, Int. J. Radiat. Biol. 66(1994) 543- 547.

6-15. A.N. Luchnik, V.M. Glaser, S.V. Shestakov, Repair of DNA double-strand breaks requires two homologous DNA duplexes, Mol. Biol. Rep. 3 (1977) 437- 442.

6-16. T. Saeki, I. Machida, S. Nakai, Genetic control of diploid recovery after γ-irradiation in the yeast Saccharomyces cerevisiae, Mutat. Res. 73 (1980) 251-265.

6-17. V.I. Korogodin, Some regularities of the post-irradiation changes in resting yeast cells, Biofizika 3 (1958) 703- 710.

6-18. M.H. Patrick, R.H. Haynes, R.B. Uretz, Dark recovery phenomenon in yeast, 1.Comparative effects with various inactivating agents, Radiat. Res. 21 (1964) 144-163.

6-19. V.G. Petin, J.K. Kim, Survival and recovery of yeast cells after combined treatments with ionizing radiation and heat, Radiat. Res. 161 (2004) 56-63.

6-20. J.K. Kim, V.G. Petin, M.D. Tkhabisimova, Survival and recovery of yeast cells after simultaneous treatment of UV light radiation and heat, Photochem. Photobiol.79 (4) (2007) 349-355.

6-21. J.K. Kim, L.N. Komarova, M.D. Tkhabisimova, V.G. Petin, Inhibition of recovery from potentially lethal damage by chemicals in Chinese hamster cells is realized through the production of irreversible damage, Korean J. Environ. Biol. 23 (4)(2005) 390-397.

6-22. E.J. Hall, Radiobiology for the Radiologist, Lippincott: Williams and Wilkins, Philadelphia, 2000.

6-23. D.V. Petin, V.G. Petin, Genetic control of RBE of α-particles for yeast cells irradiated in stationary and exponential phase of growth, Mutat. Res. 326 (1985)

211-218.

6-24. V.G. Petin, J.K. Kim, Liquid holding recovery kinetics in wild-type and radiosensitive mutants of the yeast Saccharomyces exposed to low- and high-LET radiation, Mutat. Res. 570 (2005) 1-8.

서 지 정 보 양 식			
수행기관보고서번호	위탁기관보고서번호	표준보고서번호	INIS주제코드
KAERI/RR-3749/2014			

제목/부제	방사선 복합 생물반응 연구
연구책임자 및 부서명	김진홍 (생명공학연구부)
연구자 및 부서명	김진규 (생명공학연구부), 김동호 (“), 노창현 (“), 정동민 (“), 강미영 (“), 류태호 (“), 장은영 (“)

발 행 지	대전	발행기관	한국원자력연구원	발행일	2014. 12
페 이 지	102 면	도표	유(○), 무( )	크 기	27 cm
참고사항	2014년 창의연구사업				
비밀여부	공개(○), 대외비( ), 급비밀		보고서종류	연구보고서	
연구위탁기관			계약 번호		

초록(300단어 내외)

방사선 연구개발의 국가 연구주체인 한국원자력연구원 첨단방사선연구소는 인체를 포함한 방사선 생물방호의 근간이 되는 방사선 생물선량 평가 및 반응검출 기술개발의 임무를 가지고 있다. 원자력 사고 또는 방사선 이용의 증가에 따른 대비책으로 방사선 생물방호 원천기술의 개발과 기술도약을 이루기 위한 노력을 기울여왔으며 특히, 방사선을 과학, 의학, 산업 분야 등에 이용함에 있어 생물학적 효용성을 증대시키기 위한 기술근거로서 방사선과 물리·화학적 요인의 복합작용 심화연구를 수행하여 국제적 기술우위를 확보하였다. 방사선과 다양한 물리·화학적 요인의 복합 생물반응을 검출하고 이를 응용할 수 있는 기술을 개발함으로써 국내 방사선 분야 기술우위와 국격 향상에 기여함과 동시에 국제사회의 방사선 연구 패러다임 변화와 생물방호 신개념에 부합하는 생물학적 선량평가 및 생물방호 원천기술을 확립하기 위한 연구를 수행하였다. 생물방호 및 생물선량 평가 분야에서 국제적으로 인정받는 방사선생물학 연구실로 발돋움하는데 기여하고 방사선의 과학적 이용 효율을 증대시키는 데 필요한 기술근거를 제공할 것이다.

주제명키워드 (10단어내외)	이온화 방사선, 복합작용, 생물방호, 세포반응, 복합작용

세포신호, p53, 방사선방어, 커큐민

BIBLIOGRAPHIC INFORMATION SHEET

Performing Org. Report No.	Sponsoring Org. Report No.	Standard Report No.	INIS Subject Code
KAERI/RR-3749/2014			

Title/Subtitle	Biological Responses to Combined Action of Radiation
Project Manager and Dept.	Jin-Hong Kim (Research Division for Biotechnology)
Researcher and Dept.	JK Kim (Research Division for Biotechnology), DH Kim (“). C Roh (''), DM Chung (''), MY Kang (''), TH Ryu (''), EY Jang ('')

Pub. Place	Daejeon	Pub. Org.	KAERI	Pub. Date	Jan. 2014
Page	102 pp.	Ill. and Tab.	Yes(○), No( )	Size	27 cm
Note	2014 Creative Research Project				
Classified	Open(○), Outside( ), Class		Report Type	Research Report	
Sponsoring Org.			Contract No.		

Abstract(about 300 words)

The responsibility of KAERI ARTI is to research and develop radiation technology. Strong motivation and RT-based biotechnologies necessary for the future R&D plans can be provided from the results of this research. An advanced analytical method was suggested for the combined action of ionizing radiation with another factor. Using the method, it is possible to predict in advance the maximum value of synergistic interaction and the conditions to achieve the maximum. By elaborating the present research results, new technologies will be established for analysing the combined effects of radiation with another factor and radiosensitivity of organisms. Biodosimetry techniques implemented in this research can play an important role for ARTI to be an internationally recognized radiation biology and biodosimetry laboratory. The results of this study give a clues for establishment of important technology associated with enhancing positive efficacy of radiation applications.

Subject Keywords (about 10 words): ionizing radiation, biodosimetry, combined effects

radiation protection, cell signals, p53, radiomodification, curcumin